Published in final edited form as:
Curr Drug Targets. 2008 March ; 9(3): 174–189.

Lipoprotein Size and Susceptibility to Atherosclerosis—Insights from Genetically Modified Mouse Models

Murielle M. Véniant[1,**], **Anne P. Beigneux**[2,**], **André Bensadoun**[3], **Loren G. Fong**[2], and **Stephen G. Young**[2,*]

[1] Amgen Inc., One Amgen Center Drive, Thousand Oaks, CA 91320-1799

[2] Department of Medicine/Division of Cardiology, David Geffen School of Medicine, University of California, Los Angeles, CA 90095

[3] Division of Nutritional Sciences, Cornell University, Ithaca, NY 14853

Apo-B–Containing Lipoproteins and Atherosclerosis

High plasma levels of the apo-B–containing lipoproteins are casually implicated in the pathogenesis of atherosclerotic coronary heart disease (CHD) (1). This finding, which is backed by many decades of experimental animal studies and human clinical trial data, has sparked interest in defining which classes of apo-B–containing lipoprotein particles are most atherogenic (*i.e.*, whether there are intrinsic differences in the atherogenicity of different classes of lipoprotein particles). There is overwhelming evidence that cholesterol-rich LDL, the smallest of the apo-B–containing particles, are atherogenic (1–3). Patients with familial hypercholesterolemia have a striking increase in the plasma levels of LDL and develop severe premature atherosclerosis. On the other hand, there is substantial evidence that larger lipoproteins, such as chylomicron and VLDL remnants, can also be atherogenic. For example, patients with Type III hyperlipidemia accumulate cholesterol-rich VLDL and chylomicron remnants and are susceptible to peripheral vascular disease and coronary artery disease (4,5).

Although small LDL particles and larger remnant lipoproteins both appear to be atherogenic, it has been difficult to discern which particles are the most potent in causing atherosclerosis. Human epidemiologic studies do not provide unequivocal insights, in part because many patients with coronary artery disease have increased levels of both small LDL and large VLDL, obscuring the identity of the culprit lipoproteins. Studies of human genetic diseases also have not provided unequivocal answers. Humans with familial hypercholesterolemia and Type III hyperlipidemia both have high cholesterol levels and atherosclerosis. However, even if it were possible to assemble large groups of age- and sex-matched patients with familial hypercholesterolemia and Type III hyperlipidemia, and even if the subjects were perfectly matched for plasma cholesterol levels and other atherosclerosis risk factors, it might still be difficult to determine whether LDL particles or chylomicron/VLDL remnants are the most atherogenic. One of the reasons that it would be difficult is that Type III hyperlipidemia generally develops in young adults, whereas the elevated cholesterol levels in patients with familial hypercholesterolemia are lifelong.

*To whom correspondence should be addressed: 695 Charles E. Young Dr. South, Los Angeles, CA 90095. Tel: (310) 267-4380; Fax: (310) 267-2722; sgyoung@mednet.ucla.edu.
**Contributed equally.

Atherogenicity of Large, Triglyceride-Rich Lipoproteins

Most investigators have assumed that large triglyceride-rich lipoproteins are not as atherogenic as smaller cholesterol-rich lipoproteins. Humans with deficiencies in lipoprotein lipase or apolipoprotein CII have familial chylomicronemia, frequently maintaining plasma triglyceride levels >2,000 mg/dl (6,7). These individuals also have high plasma cholesterol levels, generally more than 250 mg/dl, with nearly all of the cholesterol in large chylomicron/VLDL particles (the levels of cholesterol in the LDL and HDL fractions are typically quite low). Those who have studied patients with familial chylomicronemia have commented that these individuals are not particularly susceptible to coronary artery disease (6,7). However, opinions about this issue are not uniform. Dr. Michael Hayden's group at the University of British Columbia has challenged the concept that patients with familial chylomicronemia are protected from atherosclerosis (8). They reported four patients with familial chylomicronemia (from well characterized *LPL* mutations—mostly missense mutations yielding catalytically inactive protein) who had premature peripheral vascular disease or coronary artery disease or both. Like typical chylomicronemia patients, all four of these patients had markedly elevated plasma triglyceride levels (ranging from ~1800–4600 mg/dl), low LDL cholesterol levels (28 ± 16 mg/dl), and low HDL cholesterol levels (17 ± 7 mg/dl). Total plasma cholesterol levels were elevated (200–425 mg/dl), with nearly all of the cholesterol in the VLDL/chylomicron fraction (*i.e.*, the $d < 1.006$ g/ml lipoproteins) (8). Whether the elevated cholesterol levels within the chylomicron/VLDL fraction were responsible for the atherosclerosis in these patients is not entirely clear, but it seems likely to us that this was the case.

The atherogenicity of very large, triglyceride-rich particles has also been examined in rabbit models. More than 50 years ago, Duff and McMillan (9) found that diabetic rabbits on a high-cholesterol diet had fewer atherosclerotic lesions than nondiabetic rabbits fed the same cholesterol-rich diet. While the diabetic and nondiabetic rabbits both had severe hypercholesterolemia, the diabetic rabbits also had severe hypertriglyceridemia (plasma triglyceride levels >5000 mg/dl). The observation that hypertriglyceridemia protects diabetic cholesterol-fed rabbits from atherosclerosis was verified and examined in more detail by the laboratory of Dr. Donald Zilversmit (10,11). They proposed that the hypertriglyceridemic diabetic cholesterol-fed rabbits are protected from atherosclerosis because most of the cholesterol in these rabbits is carried in lipoproteins that are too large to enter the arterial wall. They found that the majority of the cholesterol in the diabetic rabbits was in "giant lipoproteins" with diameters >75 nm (10,12). They also found that the ability of lipoproteins to enter the arterial intima depended on size, and that the "giant lipoproteins" were "practically excluded" from the arterial wall, with an intimal clearance rate less than 5% of LDL-sized particles (10,11).

Lipoprotein Size and Atherosclerosis in Mouse Models

During the past 15 years, the mouse has become the predominant model for studying atherosclerosis. Mice are less expensive than rabbits or primates, and the ability to create transgenic and gene-knockout models has made it possible to investigate the relevance of dozens of genes in atherogenesis.

Very early after the onset of the "mouse era" in atherosclerosis research (13–16), gene-knockout models were established for both familial hypercholesterolemia (LDL receptor deficiency) (17,18) and Type III hyperlipidemia (apo-E deficiency) (19–22). Chow-fed apo-E–deficient ($Apoe^{-/-}$) mice manifest a dramatic accumulation of cholesterol-rich chylomicron/VLDL lipoproteins in the plasma, even on a low-fat chow diet, and develop advanced atherosclerotic lesions (22). LDL receptor–deficient ($Ldlr^{-/-}$) mice have mild–

moderate increases in LDL cholesterol levels on a chow diet and develop modest atherosclerotic lesions (22). Unfortunately, direct comparisons of *Apoe*$^{-/-}$ and *Ldlr*$^{-/-}$ mice shed little light on the *relative* atherogenicities of the large VLDL/LDL remnants and small LDL particles, simply because the total plasma cholesterol levels in the two mouse models are very different (~375–450 mg/dl in *Apoe*$^{-/-}$ mice *versus* only ~200–225 mg/dl in *Ldlr*$^{-/-}$ mice) (17–22). Another confounding factor is the overlapping lipoprotein sizes in the two models. *Apoe*$^{-/-}$ mice have elevated levels of LDL-sized particles, in addition to VLDL and chylomicron remnants (23–27), making it difficult to determine which lipoproteins are more important in contributing to atherosclerosis. Finally, there are significant differences in the apolipoprotein content of lipoproteins in *Apoe*$^{-/-}$ and *Ldlr*$^{-/-}$ mice. The vast majority of remnant lipoproteins in *Apoe*$^{-/-}$ mice contain apo-B48 (19–21,28), while the LDL in *Ldlr*$^{-/-}$ mice contain apo-B100 (17,28).

Modifying Lipid and Lipoprotein Phenotypes in *Apoe*$^{-/-}$ Mice with *Apob* Mutations

Lipoprotein size and susceptibility to atherosclerosis in *Apoe*$^{-/-}$ mice have been modified by rendering these mice homozygous for either the “apo-B48–only” or the “apo-B100–only” mutation in *Apob* (29). The laboratory of Dr. Stephen Young (24,29) sought to answer a question that had vexed the lipoprotein/atherosclerosis field for several decades: Are the two different apo-B proteins, apo-B48 and apo-B100, intrinsically different in their abilities to cause atherosclerosis? The two apo-B isoforms differ in size by more than 2400 amino acids (98, 99), and it seemed plausible that they might differ in their metabolism within the arterial wall and differ in their ability to induce atherosclerosis. To test this issue, Dr. Young’s laboratory analyzed susceptibility to atherosclerosis in mice that synthesize exclusively apo-B48 (*Apob*$^{48/48}$ mice) or apo-B100 (*Apob*$^{100/100}$ mice) (27). The *Apob*$^{48/48}$ mice were generated by using “pop-in, pop-out” gene targeting to insert a TGA stop codon into codon 2153 of the mouse apo-B gene. *Apob*$^{100/100}$ mice were produced by inserting a CTA-leucine codon into codon 2153 of the mouse apo-B gene (28). Even when the CTA-leucine codon is edited to UTA by the apo-B RNA-editing machinery (30), no stop codon is generated, as UTA also specifies leucine.

The *Apob*$^{48/48}$ and *Apob*$^{100/100}$ mice were crossed with *Apoe*$^{-/-}$ mice to produce apo-E–deficient apo-B48–only mice (*Apoe*$^{-/-}$*Apob*$^{48/48}$) and apo-E–deficient apo-B100–only mice (*Apoe*$^{-/-}$*Apob*$^{100/100}$) (27). When the *Apoe*$^{-/-}$*Apob*$^{48/48}$ mice were fed a chow diet, their total and LDL cholesterol levels were somewhat higher than in *Apoe*$^{-/-}$*Apob*$^{+/+}$ mice (24). The total and LDL cholesterol levels in the *Apoe*$^{-/-}$*Apob*$^{100/100}$ mice were significantly lower than in *Apoe*$^{-/-}$*Apob*$^{+/+}$ mice (24). The lower LDL levels in *Apoe*$^{-/-}$*Apob*$^{100/100}$ mice are almost certainly due to the fact that the apo-B100–containing LDL can be removed from the plasma by the LDL receptor (27,28), while apo-B48–containing lipoproteins in *Apoe*$^{-/-}$*Apob*$^{+/+}$ mice cannot be removed by this pathway. As illustrated in Figure 1, the vast majority of the plasma cholesterol in the *Apoe*$^{-/-}$*Apob*$^{100/100}$ mice is located in the VLDL fraction; consequently, these mice have been dubbed “VLDL-cholesterol mice” (24–26).

We examined large groups of *Apoe*$^{-/-}$*Apob*$^{+/+}$, *Apoe*$^{-/-}$*Apob*$^{48/48}$, and *Apoe*$^{-/-}$*Apob*$^{100/100}$ mice (24). While the mean plasma cholesterol levels in the three groups of mice differed significantly, the cholesterol levels in individual mice actually overlapped considerably. We therefore were curious to determine whether, at a given cholesterol level, mice expressing exclusively apo-B48 (*Apoe*$^{-/-}$*Apob*$^{48/48}$ mice) had fewer (or more) atherosclerotic lesions than mice expressing exclusively apo-B100 (*Apoe*$^{-/-}$*Apob*$^{100/100}$ mice). Therefore, after 7 months on a regular chow diet, all of the *Apoe*$^{-/-}$*Apob*$^{+/+}$, *Apoe*$^{-/-}$*Apob*$^{48/48}$, and *Apoe*$^{-/-}$*Apob*$^{100/100}$ mice were euthanized and perfusion-fixed. Atherosclerosis was

measured by pinning out the aorta and then using computer-assisted morphometric techniques to quantify the percentage of the aortic surface covered by atherosclerotic lesions. Most of the lesions in all three groups of mice were located in the ascending aorta and aortic arch. Atherosclerosis was more extensive in the *Apoe*$^{-/-}$*Apob*$^{48/48}$ mice, and less extensive in the *Apoe*$^{-/-}$*Apob*$^{100/100}$ mice, compared with the *Apoe*$^{-/-}$*Apob*$^{+/+}$ mice (27). Once again, however, a considerable amount of overlap existed. Importantly, the amount of atherosclerosis correlated with total plasma cholesterol levels in all three groups of mice. Also, all three groups appeared to fall on the same "total cholesterol *vs.* atherosclerosis curve." In other words, the *Apoe*$^{-/-}$*Apob*$^{+/+}$, *Apoe*$^{-/-}$*Apob*$^{48/48}$, and *Apoe*$^{-/-}$*Apob*$^{100/100}$ mice had similar amounts of atherosclerosis when their total cholesterol levels were similar. From this study, Dr. Young's group concluded that the total cholesterol level appeared to be the most important factor in the development of atherosclerosis and that there did not appear to be any significant differences between the intrinsic abilities of apo-B48– and apo-B100–containing lipoproteins to promote atherosclerosis (24). There was no relationship between plasma triglyceride levels and atherosclerotic lesions.

Lipoprotein Size and Atherosclerosis in *Apoe*$^{-/-}$ and *Ldlr*$^{-/-}$ Mice After "Evening Up" the Plasma Cholesterol Levels

Ldlr$^{-/-}$ mice do not develop severe hypercholesterolemia because their livers synthesize abundant amounts of apo-B48, and apo-B48–containing lipoproteins can be efficiently cleared independently of the LDL receptor (27,28). We predicted that it would be possible to increase LDL levels in *Ldlr*$^{-/-}$ mice by eliminating apo-B48 synthesis. To test this idea, we bred *Ldlr*$^{-/-}$*Apob*$^{100/100}$ mice (27). As predicted, these mice had significantly higher plasma cholesterol levels than the *Ldlr*$^{-/-}$*Apob*$^{+/+}$ mice, and essentially all of the cholesterol in their plasma was located in the LDL, as judged by fractionation of the plasma by fast phase liquid chromatography (FPLC) (Figure 1). We have dubbed the *Ldlr*$^{-/-}$*Apob*$^{100/100}$ mice "LDL-cholesterol mice" (25–27). The distribution of cholesterol in these "LDL cholesterol mice" was strikingly different from those of the "VLDL cholesterol mice" (*Apoe*$^{-/-}$*Apob*$^{100/100}$) (Figure 1). Of note, the total plasma cholesterol levels in the *Apoe*$^{-/-}$*Apob*$^{100/100}$ and the *Ldlr*$^{-/-}$*Apob*$^{100/100}$ mice were virtually identical (25). HDL cholesterol levels were also indistinguishable (25). The triglyceride levels were somewhat higher in *Apoe*$^{-/-}$*Apob*$^{100/100}$ mice than in *Ldlr*$^{-/-}$*Apob*$^{100/100}$ mice (25).

While the total plasma cholesterol levels in *Apoe*$^{-/-}$*Apob*$^{100/100}$ and *Ldlr*$^{-/-}$*Apob*$^{100/100}$ mice were very similar, the size of the lipoprotein particles in the two models was not (25). Nearly all of the cholesterol in the plasma of *Apoe*$^{-/-}$*Apob*$^{100/100}$ mice was in the VLDL, whereas nearly all of the cholesterol in the *Ldlr*$^{-/-}$*Apob*$^{100/100}$ mice was in the LDL (Figure 1). The diameters of the lipoproteins were determined by dynamic light scattering analysis with a Microtrac Series 150 Ultrafine particle analyzer. We found that the lipoproteins in the plasma of *Apoe*$^{-/-}$*Apob*$^{100/100}$ mice were actually quite large (mean size of 63 nm) whereas the vast majority of lipoproteins in *Ldlr*$^{-/-}$*Apob*$^{100/100}$ mice were small (mean size of 24 nm) (Figure 2) (25). Indeed, there was almost no overlap in the sizes of the apo-B–containing lipoproteins in the plasma. Finding identical cholesterol levels but differences in lipoprotein size implied that the numbers of particles in the plasma of the two models would be different. Indeed, this was the case. Plasma apo-B100 levels were nearly fourfold higher in *Ldlr*$^{-/-}$*Apob*$^{100/100}$ mice than in *Apoe*$^{-/-}$*Apob*$^{100/100}$ mice (Figure 3) (25). Thus, we had created two hypercholesterolemic mouse models—both "apo-B100–only" and both with the same plasma cholesterol levels—but with striking differences in lipoprotein sizes and lipoprotein numbers (25).

To obtain insights into the relative atherogenicities of two very different lipoprotein phenotypes, we examined susceptibility to atherosclerosis in *Apoe*$^{-/-}$*Apob*$^{100/100}$ and

Ldlr$^{-/-}$*Apob*$^{100/100}$ mice (25). For controls, we analyzed *Apoe*$^{-/-}$ and *Ldlr*$^{-/-}$ mice that were homozygous for a wild-type apo-B allele (*Apoe*$^{-/-}$*Apob*$^{+/+}$ and *Ldlr*$^{-/-}$*Apob*$^{+/+}$ mice). All four groups of mice ($n \geq 40$/group) were fed a chow diet for 40 weeks. At the 40-week time point, the total plasma cholesterol levels (mean ± S.D.) in *Apoe*$^{-/-}$*Apob*$^{100/100}$ and *Ldlr*$^{-/-}$*Apob*$^{100/100}$ were virtually identical (334 ± 12 and 336 ± 8 mg/dl, respectively). As expected, the total plasma cholesterol levels were higher in *Apoe*$^{-/-}$*Apob*$^{+/+}$ mice (497 ± 23 mg/dl) and lower in *Ldlr*$^{-/-}$*Apob*$^{+/+}$ mice (235 ± 12 mg/dl) (25).

Computer-assisted morphometric techniques were used to assess the percent of the aortic surface covered by atherosclerotic lesions at 40 weeks (25). The results were unequivocal. Mice with larger numbers of small lipoproteins (*i.e.*, the *Ldlr*$^{-/-}$*Apob*$^{100/100}$ mice) had far more atherosclerosis than mice with smaller numbers of large lipoproteins (*i.e.*, the *Apoe*$^{-/-}$*Apob*$^{100/100}$ mice) (14.0 ± 0.46% *versus* only 4.8 ± 0.37% of the aortic surface; $P < 0.0001$) (Figure 4) (25). Of note, *Apoe*$^{-/-}$*Apob*$^{+/+}$ mice actually had only about one-half as much atherosclerosis (7.47 ± 0.67% of the aortic surface) as *Ldlr*$^{-/-}$*Apob*$^{100/100}$ mice, despite having far higher plasma cholesterol levels. As expected, the *Ldlr*$^{-/-}$*Apob*$^{+/+}$ mice had minimal atherosclerosis (0.41 ± 0.16%, ~3% of that in *Ldlr*$^{-/-}$*Apob*$^{100/100}$ mice; $P < 0.0001$) (25). The *Ldlr*$^{-/-}$*Apob*$^{100/100}$ mice were far more susceptible to atherosclerosis than *Apoe*$^{-/-}$*Apob*$^{100/100}$ mice. Representative pinned-out aortas from all four genotypes of mice (*Apoe*$^{-/-}$*Apob*$^{+/+}$, *Apoe*$^{-/-}$*Apob*$^{100/100}$, *Ldlr*$^{-/-}$*Apob*$^{+/+}$, *Ldlr*$^{-/-}$*Apob*$^{100/100}$) are shown in Figure 5 (25). The microscopic appearance of the atherosclerotic lesions in the proximal aortas was similar in the different groups (Figure 6) (25).

When we plotted atherosclerotic lesion measurements and total cholesterol levels in *Ldlr*$^{-/-}$*Apob*$^{100/100}$ and *Apoe*$^{-/-}$*Apob*$^{100/100}$ mice, we found that *Ldlr*$^{-/-}$*Apob*$^{100/100}$ mice had far more atherosclerosis than *Apoe*$^{-/-}$*Apob*$^{100/100}$ mice with similar total cholesterol levels (Figure 7) (25). A plot of atherosclerotic lesions and plasma apo-B100 levels (Figure 7) revealed that *Ldlr*$^{-/-}$*Apob*$^{100/100}$ mice—the group with the highest apo-B100 levels—had the most atherosclerosis.

We also measured the amount of free and esterified cholesterol in the aortas and the rate of aortic DNA synthesis. The *Ldlr*$^{-/-}$*Apob*$^{100/100}$ mice accumulated far more cholesterol in their aortas than the *Apoe*$^{-/-}$*Apob*$^{100/100}$ mice, despite almost identical plasma cholesterol levels (25) (Figure 8). We found a strong positive correlation between lesion size, measured morphometrically, and the aortic content of esterified cholesterol, both for all of the mice in the study ($r = 0.858$; $P < 0.0001$) and for most of the subgroups (*Apoe*$^{-/-}$*Apob*$^{+/+}$: $r = 0.719$, $P < 0.0001$; *Apoe*$^{-/-}$*Apob*$^{100/100}$: $r = 0.705$, $P < 0.0001$; and *Ldlr*$^{-/-}$*Apob*$^{100/100}$: $r = 0.734$, $P < 0.0001$) (25).

To measure DNA synthesis within the aortas, we administered $^{2}H_2O$ to the mice and then assessed, by mass spectrometry, the incorporation of deuterium into newly synthesized DNA (25). The aortic DNA synthesis rate in the experimental animals was high; nearly 10–12% of the cells in the aorta had divided during the three weeks prior to euthanizing the mice (25). The correlation between lesions, as assessed by morphometry, and the aortic DNA synthesis rate was moderate ($r = 0.574$, $P < 0.0001$). The correlation between the aortic cholesterol content and the aortic DNA synthesis rate was lower ($r = 0.482$, $P < 0.0001$ for free cholesterol; $r = 0.469$, $P < 0.0001$ for esterified cholesterol). In line with the morphometric results and the cholesterol measurements, the aortic DNA synthesis in the *Ldlr*$^{-/-}$*Apob*$^{100/100}$ mice was almost twice as high as in *Apoe*$^{-/-}$*Apob*$^{100/100}$ mice (Figure 8) (25).

The total plasma cholesterol levels in *Apoe*$^{-/-}$*Apob*$^{100/100}$ and *Ldlr*$^{-/-}$*Apob*$^{100/100}$ mice are virtually identical, and the principal structural protein of lipoprotein particles, apo-B100, is

the same in both models (25). While there are several potential explanations for these results, we believe that the most likely explanation is the differences in the lipoprotein phenotype, with large numbers of small lipoproteins (as in *Ldlr*$^{-/-}$*Apob*$^{100/100}$ mice) being more atherogenic than lower numbers of large lipoproteins (as in *Apoe*$^{-/-}$*Apob*$^{100/100}$ mice) (Figure 9) (25,26). Of note, more than half of the cholesterol in *Apoe*$^{-/-}$*Apob*$^{100/100}$ mice was contained in "giant" lipoproteins with diameters greater than 70 nm—the types of particles that have little ability to penetrate the arterial wall (10).

Interpreting the Differences in Atherosclerotic Lesions in *Apoe*$^{-/-}$*Apob*$^{100/100}$ and *Ldlr*$^{-/-}$*Apob*$^{100/100}$ Mice

The total plasma cholesterol levels in *Apoe*$^{-/-}$*Apob*$^{100/100}$ and *Ldlr*$^{-/-}$*Apob*$^{100/100}$ mice were almost identical, but lipoprotein sizes were not. The striking differences in the sizes of cholesterol-carrying particles, given nearly equivalent plasma cholesterol levels, was explained by differences in the numbers of apo-B–containing lipoprotein particles in the plasma (25). Plasma levels of apo-B100 were almost fourfold higher in *Ldlr*$^{-/-}$*Apob*$^{100/100}$ mice.

Figure 9 shows the mean values for atherosclerotic lesions and cholesterol levels for each of the four genotypes of mice. These data suggest that susceptibility to atherosclerosis changes according to lipoprotein size. Thus, there appears to be a distinct "plasma cholesterol *versus* atherosclerosis" relationship for lipoproteins of different sizes. When most of the lipoproteins are small (*i.e.*, in the LDL size range), as in the two groups of LDL receptor–deficient mice, changing the plasma cholesterol levels from ~200 to ~300 mg/dl resulted in a nearly 30-fold increase in amount of atherosclerotic lesions in the aorta (25). When most of the cholesterol was located within large lipoprotein particles (*i.e.*, VLDL-sized particles), as in the *Apoe*$^{-/-}$*Apob*$^{100/100}$ and *Apoe*$^{-/-}$*Apob*$^{+/+}$ mice, increasing the plasma cholesterol level by ~150 mg/dl increased atherosclerotic lesions by less than twofold (25).

We believe that the very steep increase in lesions with relatively small changes in LDL levels is consistent with earlier findings in mouse models. Previously, we generated human apo-B transgenic mice (31) and examined their susceptibility to atherosclerotic lesions on a high-fat diet (32). The human apo-B transgene had little impact on the concentration of VLDL-IDL particles in the plasma, but increased LDL cholesterol levels (by ~80 mg/dl). This rather small increase in the concentration of LDL in the plasma was associated with a greater than 10-fold increase in the extent of atherosclerotic lesions (32). Similarly, increasing LDL levels in *Apobec1* knockout mice (by rendering them homozygous for *Ldlr* deficiency) resulted in a striking increase in atherosclerosis (33). A steep "atherosclerosis *versus* LDL cholesterol slope" is probably not unique to mouse models. In humans, where most of the cholesterol is in LDL particles, doubling plasma cholesterol levels increases the risk of coronary disease sixfold (34).

It is possible, of course, that factors other than lipoprotein size and apo-B concentration could have affected atherogenesis in *Ldlr*$^{-/-}$*Apob*$^{100/100}$ and *Apoe*$^{-/-}$*Apob*$^{100/100}$ mice (25,26). For example, apo-E in the lipoproteins of *Ldlr*$^{-/-}$*Apob*$^{100/100}$ mice might somehow increase the binding of lipoproteins to proteoglycans within the arterial wall, thereby accelerating atherogenesis. Similarly, the apo-AIV-enrichment of VLDL in *Apoe*$^{-/-}$*Apob*$^{100/100}$ mice might have had the opposite effect. Alternatively, perhaps the LDL in the *Ldlr*$^{-/-}$*Apob*$^{100/100}$ mice was more susceptible to oxidation because of a longer residence time in the plasma, leading to more atherosclerosis. Also, the macrophages in *Ldlr*$^{-/-}$*Apob*$^{100/100}$ mice obviously retain the capacity to produce apo-E, while those in *Apoe*$^{-/-}$*Apob*$^{100/100}$ mice do not. Bone marrow transplantation studies have suggested that the local production of apo-E within macrophages in the arterial wall can limit the

progression of lesions (35). However, this "anti-atherogenic role of apo-E in the arterial wall" would seemingly not explain our findings, given that the mice with the capacity to synthesize apo-E (*e.g.*, $Ldlr^{-/-}Apob^{100/100}$ mice) had *more* atherosclerosis, not less.

Studies with $Ldlr^{-/-}Apob^{100/100}$ and $Apoe^{-/-}Apob^{100/100}$ Mice That Are Also Homozygous for the Obesity (*Ob*) Mutation

$Apoe^{-/-}$ and $Ldlr^{-/-}$ mice are useful models for examining hyperlipidemia and atherosclerosis, but unlike many human patients with coronary artery disease, they are neither insulin-resistant nor diabetic. To develop mouse models that exhibit both insulin resistance and hyperlipidemia, we bred $Apoe^{-/-}Apob^{100/100}ob^{-/-}$ and $Ldlr^{-/-}Apob^{100/100}ob^{-/-}$ mice. As expected, the body weights of the $Apoe^{-/-}Apob^{100/100}ob^{-/-}$ and $Ldlr^{-/-}Apob^{100/100}ob^{-/-}$ mice were far greater than those of wild-type mice (Figure 10). Postprandial blood glucose levels were significantly elevated only in the $Apoe^{-/-}Apob^{100/100}ob^{-/-}$ mice (Figure 11A). However, both $Apoe^{-/-}Apob^{100/100}ob^{-/-}$ and $Ldlr^{-/-}Apob^{100/100}ob^{-/-}$ mice had marked hyperinsulinemia ($P < 0.0001$ *vs*. wild-type C57BL/6 mice, Figure 11B). The plasma insulin levels in $Apoe^{-/-}Apob^{100/100}ob^{-/-}$ were greater than those of $Ldlr^{-/-}Apob^{100/100}ob^{-/-}$ (>50 ng/ml in the former mice and 30–40 ng/ml in the latter; Figure 11B).

By 11–12 weeks of age, both $Apoe^{-/-}Apob^{100/100}ob^{-/-}$ and $Ldlr^{-/-}Apob^{100/100}ob^{-/-}$ mice were hypertensive, compared with wild-type C57BL/6 mice (data not shown). Previously, it has been demonstrated that $Apoe^{-/-}$ mice exhibit hypertension by 7.5 months of age, while no hypertension was found at 6 weeks of age (36). Also, hypertension has been observed in $Ldlr^{-/-}ob^{-/-}$ mice when the blood pressure was measured with a telemetric system (37).

From 7–8 weeks to 15–16 weeks of age, the total cholesterol levels of $Apoe^{-/-}Apob^{100/100}ob^{-/-}$ and $Ldlr^{-/-}Apob^{100/100}ob^{-/-}$ mice oscillated between 850 and 1,100 mg/dl, almost tenfold higher than in wild-type C57BL/6 mice (Figure 12A, $P < 0.001$). There were no significant differences in cholesterol levels between $Apoe^{-/-}Apob^{100/100}ob^{-/-}$ and $Ldlr^{-/-}Apob^{100/100}ob^{-/-}$ mice at any age; however, when the plasma lipoproteins were fractionated on an HPLC system, the distributions of VLDL, LDL, and HDL were quite different. HDL carried most of the cholesterol in wild-type C57BL/6 mice, consistent with published observations (38) (Figure 12B). $Ldlr^{-/-}Apob^{100/100}ob^{-/-}$ mice had more cholesterol in LDL than in VLDL or HDL; $Apoe^{-/-}Apob^{100/100}ob^{-/-}$ mice had more cholesterol in VLDL than in LDL or HDL (Figure 12B). HDL levels in $Apoe^{-/-}Apob^{100/100}ob^{-/-}$ and $Ldlr^{-/-}Apob^{100/100}ob^{-/-}$ mice were identical.

Plasma triglyceride levels in $Apoe^{-/-}Apob^{100/100}ob^{-/-}$ and $Ldlr^{-/-}Apob^{100/100}ob^{-/-}$ mice were three- and three- to five-fold higher**,** respectively, than those in wild-type C57BL/6 mice (Figure 12C, $P < 0.0001$ for both). The plasma free fatty acid levels were elevated in both $Apoe^{-/-}Apob^{100/100}ob^{-/-}$ and $Ldlr^{-/-}Apob^{100/100}ob^{-/-}$ mice ($P < 0.0004$ for both groups compared with wild-type C57BL/6 mice) (data not shown).

Quantitative measurements of atherosclerosis revealed that $Ldlr^{-/-}Apob^{100/100}ob^{-/-}$ mice (Figure 13A) had significantly more lesions $Apoe^{-/-}Apob^{100/100}ob^{-/-}$ mice (21.5 ± 5.4% of the surface of the aorta vs. 12.3 ± 3.7%), despite having virtually identical total cholesterol levels. Again, these findings are consistent with a greater atherogenicity of large numbers of LDL particles. Representative examples of lesions in $Apoe^{-/-}Apob^{100/100}ob^{-/-}$ and $Ldlr^{-/-}Apob^{100/100}ob^{-/-}$ mice are shown in Figure 13B.

A New Model That Might Ultimately Prove Useful to Analyze the Impact of Lipoprotein Size on Atherosclerosis—GPIHBP1 Knockout Mice

During the past year, Drs. Young, Fong, Bensadoun, and Beigneux investigated a new knockout mouse that could ultimately yield new insights into the relationship between lipoprotein size and atherogenesis. They found that mice lacking glycosylphosphatidylinositol-anchored high density lipoprotein-binding protein 1 (GPIHBP1) have chylomicronemia, with extraordinarily large apo-B–containing lipoprotein particles (39). It is now clear that GPIHBP1 plays a critical role in the lipolytic processing of apo-B–containing lipoproteins in the plasma. *Gpihbp1*-deficient (*Gpihbp1*$^{-/-}$) mice on a chow diet have severe chylomicronemia, with grossly milky plasma (Figure 14) and plasma triglyceride levels of 2000–5000 mg/dl. *Gpihbp1* is expressed at high levels in heart and adipose tissue and moderate levels in skeletal muscle—very similar to the pattern of expression for lipoprotein lipase (LpL). By immunohistochemistry, GPIHBP1 is located exclusively on the luminal face of endothelial cells, the site where lipolysis of triglyceride-rich lipoproteins is known to occur. Also, cultured cells that have been transfected with a *Gpihbp1* cDNA bind both chylomicrons and LpL. Because GPIHBP1 binds both LpL and chylomicrons and because *Gpihbp1*$^{-/-}$ mice develop severe chylomicronemia, we suspect that GPIHBP1 is a physiologically significant “platform” for triglyceride hydrolysis within capillaries (39).

Very preliminary observations suggest that chow-fed *Gpihbp1*$^{-/-}$ mice have an increased susceptibility to atherosclerosis (Mr. Michael Weinstein, Drs. Liya Yan, Loren Fong, unpublished observations). Should this preliminary finding hold up, this new model could prove to be useful in exploring the impact of lipoprotein size on atherogenesis.

Initial Identification of GPIHBP1 as a Molecule with Potential Relevance to Lipid Metabolism

Ioka *et al.* (40) used an expression cloning strategy to identify cDNAs (from an hepatic cDNA library) that rendered CHO cells capable of binding fluorescently labeled HDL. One of the cDNAs encoded scavenger receptor class B, type 1 (SR-BI)—a predictable result. The other cDNA encoded GPIHBP1. GPIHBP1 (228 amino acids in length) consists of an amino-terminal signal sequence, a domain rich in acidic amino acids (17 of 25 residues in the mouse sequence, and 21 of 25 in the human sequence, are glutamate or aspartate), an Ly-6 motif containing multiple cysteines, and a carboxyl-terminal hydrophobic domain that is ultimately replaced by a GPI anchor (40). The GPI anchor, which tethers GPIHBP1 to the surface of the cell, can be cleaved by a phosphatidylinositol-specific phospholipase C (PIPLC) (40). Like SR-BI (41,42), GPIHBP1 was reported to mediate the selective uptake of lipids. Excess unlabeled HDL reduced the binding of ^{125}I-HDL to GPIHBP1. The authors concluded that GPIHBP1 was probably involved in cellular cholesterol transport (40).

By northern blot, GPIHBP1 transcripts were reported to be most abundant in the heart (40). By *in situ* hybridization, Ioka *et al.* (40) found GPIHBP1 expression in cardiac muscle cells, hepatic Kupffer cells, the sinusoidal endothelium of the liver, the bronchial epithelium, and pulmonary alveolar macrophages. However, our immunohistochemical studies (39) have shown that *Gpihbp1* is expressed exclusively in endothelial cells, mainly in heart, skeletal muscle, and adipose tissue. Moreover, chylomicronemia is the only obvious phenotype in *Gpihbp1*$^{-/-}$ mice (39).

Gpihbp1$^{-/-}$ Mice Are Severely Hypertriglyceridemic on a Chow Diet

Our group studied the functional importance of GPIHBP1 in lipoprotein metabolism by examining the phenotype of *Gpihbp1*$^{-/-}$ mice. *Gpihbp1*$^{-/-}$ mice were produced by eliminating all of the exons and introns of *Gpihbp1*; northern and western blots of tissues from *Gpihbp1*$^{-/-}$ mice showed a complete absence of *Gpihbp1* expression (39).

Both male and female *Gpihbp1*$^{-/-}$ mice had milky plasma on a regular chow diet (Figure 14). This phenotype was invariably quite striking by 10 weeks of age. The plasma triglyceride levels were significantly elevated at all ages; nearly all mice had plasma triglyceride levels >1500 mg/dl at 7–10 weeks (Figure 15), and some had levels as high as 9000 mg/dl (39) (unpublished observations). Plasma cholesterol levels were also elevated in *Gpihbp1*$^{-/-}$ mice, with most ranging between 250 mg/dl and 500 mg/dl, with an occasional animal having a cholesterol level greater than 800 mg/dl (39). The plasma lipid levels in *Gpihbp1*$^{+/-}$ and *Gpihbp1*$^{+/+}$ mice were indistinguishable. To define the distribution of lipids within the plasma lipoprotein fractions, plasma lipoproteins were fractionated by size on an FPLC column. The vast majority of the triglycerides and cholesterol in the *Gpihbp1*$^{-/-}$ mice was located in large lipoproteins (*i.e.*, in the “chylomicron/VLDL” peak) (Figure 16). The diameters of the triglyceride-rich lipoproteins in *Gpihbp1*$^{-/-}$ mice were far larger than those of wild-type mice, as judged by a dynamic laser light scattering technique (Figure 17) (39). The median diameter of lipoproteins in *Gpihbp1*$^{-/-}$ mice was >150% larger than that of *Gpihbp1*$^{+/+}$ mice, and >15% of the particles in the plasma of *Gpihbp1*$^{-/-}$ mice had diameters of >122 nm (Figure 17). The FPLC fractionation studies revealed that the HDL cholesterol levels in *Gpihbp1*$^{-/-}$ mice were low (Figure 16) (43, 44).

The phenotype of *Gpihbp1*$^{-/-}$ mice differs significantly from mice lacking lipoprotein lipase (*Lpl*$^{-/-}$). *Lpl*$^{-/-}$ mice die within 24 h after birth (45,46) with triglyceride levels as high as 20,000 mg/dl (45). The cause of death in newborn *Lpl*$^{-/-}$ pups is not known with certainty, but is presumed to be due to either ischemia (from chylomicrons clogging the circulation) or starvation (due to the inability to utilize lipid nutrients in milk). A small percentage of *Lpl*$^{-/-}$ pups can be rescued by injecting the pups with an adenovirus encoding LpL (44). Following the injection of the LpL adenovirus, LpL is expressed in the liver; however, the expression of LpL falls rapidly and is absent after a few weeks. This transient expression of LpL allows some *Lpl*$^{-/-}$ pups to survive the suckling phase, and those mice can then survive on a regular chow diet for up to two years. Interestingly, the adult *Lpl*$^{-/-}$ mice had plasma triglyceride levels of 2000–4000 mg/dl on a chow diet—very similar to the triglyceride concentrations in chow-fed *Gpihbp1*$^{-/-}$ mice (44). The similarity in plasma triglyceride levels between rescued *Lpl*$^{-/-}$ mice and *Gpihbp1*$^{-/-}$ mice has led us to suspect that very little lipolytic processing occurs in the absence of GPIHBP1 even though they have respectable levels of LpL in the plasma following an injection of heparin.

Gpihbp1$^{-/-}$ Mice Have High Levels of Apo-B48 in the Plasma

The plasma lipoproteins of *Gpihbp1*$^{-/-}$ mice contain high levels of apo-B48, as judged by SDS-polyacrylamide gel electrophoresis (47). Western blots on whole plasma samples confirmed this finding (Figure 18). Of note, plasma apo-B100 levels did not appear to be perturbed in *Gpihbp1*$^{-/-}$ mice.

Thus far, the assessment of apo-B isoforms in the plasma of *Gpihbp1*$^{-/-}$ mice has been qualitative. We have not measured apo-B48 or apo-B100 concentrations, nor do we know how the amount of apo-B48 and apo-B100 in the plasma of these mice compares with those observed in *Apoe*$^{-/-}$ and *Ldlr*$^{-/-}$ mice. At this point, we do not know for sure whether the accumulation of apo-B48 is largely due to intestinal particles. Also, we do not know whether

the apparently normal amounts of apo-B100 mean that apo-B100–containing particles can be processed without GPIHBP1.

There are several potential explanations for the striking increases in apo-B48 in the plasma of *Gpihbp1*$^{-/-}$ mice. One is that apo-B48–containing chylomicrons are very large lipoproteins, and it is mainly the large lipoproteins that accumulate when lipolysis is defective. Another is that GPIHBP1 plays a specialized role in the clearance of apo-B48–containing lipoproteins, either by binding directly to apo-B48 or indirectly by binding to other apolipoproteins on those particles. In the future, we hope to assess the impact of *Gpihbp1* deficiency in mice that express exclusively apo-B100. If *Gpihbp1*$^{-/-}$*Apob*$^{100/100}$ mice do not exhibit hyperlipidemia or a striking accumulation of apo-B100 in the plasma, it would suggest that GPIHBP1 plays a special role in the metabolism of apo-B48–containing lipoproteins.

Mild Hypertriglyceridemia in *Gpihbp1*$^{-/-}$ Mice During the Suckling Phase

Gpihbp1$^{-/-}$ pups did not exhibit perinatal lethality (39), unlike the situation with newborn *Lpl*$^{-/-}$ pups (45). We recently examined the plasma lipid levels in suckling *Gpihbp1*$^{-/-}$ and *Gpihbp1*$^{+/+}$ mice; the *Gpihbp1*$^{-/-}$ pups had far higher lipid levels ($P < 0.001$), but their triglyceride and cholesterol levels remained <250 mg/dl. In contrast, suckling *Lpl*$^{-/-}$ pups had plasma triglyceride levels >20,000 mg/dl (45). We do not yet understand the mechanisms for the low lipid levels in suckling *Gpihbp1*$^{-/-}$ mice, but we are intrigued by the fact that the suckling phase of mouse development is associated with high levels of *Lpl* expression in the liver (48). We suspect that *Lpl* expression in the liver underlies the milder-than-expected hyperlipidemia in *Gpihbp1*$^{-/-}$ mice during the suckling phase.

Markedly Delayed Clearance of Retinyl Palmitate in *Gpihbp1*$^{-/-}$ Mice

After oral administration of retinyl palmitate, retinyl esters are packaged into chylomicrons in the intestine and enter the circulation. Once the particles are taken up, the retinyl esters are not re-secreted. Thus, their disappearance from the plasma reflects the rate of chylomicron clearance. In wild-type mice, the retinyl esters peak quickly (within 1–3 h), and retinyl esters are almost absent from the plasma after 10 h. In *Gpihbp1*$^{-/-}$ mice, the plasma levels of retinyl esters are >10-fold higher than those in *Gpihbp1*$^{+/+}$ mice, and the high levels of retinyl esters persist in the plasma for more than 24 h (Figure 19) (39). Given the profound delay in the clearance of retinyl palmitate in *Gpihbp1*$^{-/-}$ mice, we suspect that many other lipids would also have a prolonged circulation time in these mice. For example, we suspect that oxidized lipids in the diet would be absorbed by *Gpihbp1*$^{-/-}$ mice and then circulate for many hours or days. If so, they conceivably could contribute to the development of atherosclerotic lesions.

GPIHBP1 Is Located on the Luminal Face of the Capillary Endothelium of Tissues That Process Triglyceride-Rich Lipoproteins

When confronted with the finding of chylomicronemia in mice lacking a GPI-anchored cell-surface protein, we thought that there was only one plausible hypothesis—that GPIHBP1 is somehow involved in the LpL-mediated processing of triglyceride-rich lipoproteins along the luminal face of capillary endothelial cells. In support of this general concept, we found that GPIHBP1 is expressed highly in heart, adipose tissue, and skeletal muscle (39)—the very same tissues that express high levels of LpL and CD36, a fatty acid transporter (49). In addition, confocal immunofluorescence microscopy revealed that GPIHBP1 is found along the luminal surface of endothelial cells in both the heart and brown adipose tissue (39)

(Figure 20). GPIHBP1 is also expressed within capillaries of skeletal muscle, but it is not expressed at significant levels in capillaries of the brain (39).

Reduced Levels of LpL in the Postheparin Plasma of *Gpihbp1*$^{-/-}$ Mice

We separated LpL and hepatic lipase (HL) in postheparin plasma by heparin-sepharose chromatography and then quantified HL and LpL activities. In four experiments, LpL activity was ~20–70% lower in *Gpihbp1*$^{-/-}$ mice than wild-type mice, and the LpL:HL ratio in the *Gpihbp1*$^{-/-}$ mice was reduced by ~35–90% ($P = 0.03$) (39). We also used a mouse LpL–specific ELISA to measure LpL mass in whole plasma (following an injection of heparin). The mean postheparin LpL protein mass was significantly lower in *Gpihbp1*$^{-/-}$ mice than in wild-type control mice (175 ± 111 *vs.* 581 ± 98 ng/ml; $P < 0.001$) (39). In contrast, the levels of LpL mass in the preheparin plasma samples were similar in wild-type and *Gpihbp1*$^{-/-}$ mice. At this point in our studies, we face a conundrum: *Gpihbp1*$^{-/-}$ mice have a respectable amount of enzymatically active LpL in the plasma after an injection of heparin, yet there is seemingly almost no lipolysis of the triglyceride-rich lipoproteins. How can this be explained? We do not know the answer to this question, but we speculate that the LpL that is released by heparin in *Gpihbp1*$^{-/-}$ mice is released from pools of LpL that are not directly relevant to lipoprotein lipolysis (39).

GPIHBP1 Binds Both LpL and Chylomicrons

Because *Gpihbp1*$^{-/-}$ mice exhibit striking chylomicronemia, we hypothesized that GPIHBP1 likely functions as a binding site—along the capillary endothelium—for LpL or chylomicrons or both (39). The fact that GPIHBP1 contains a strongly negatively charged domain lent some plausibility to this hypothesis, since LpL and several apolipoproteins within chylomicrons contain positively charged domains (and since those positively charged domains are known to mediate both protein–protein and protein-heparan sulfate interactions) (2,50). To explore this possibility, we constructed a full-length mouse *Gpihbp1* cDNA expression vector (39). When we transfected LDL receptor–deficient CHO cells with the *Gpihbp1* expression vector, we observed high levels of GPIHBP1 expression at the cell surface, as judged by immunocytochemistry. Importantly, we found that this cell-surface GPIHBP1 could be released with PIPLC (39). To assess the ability of GPIHBP1 to bind LpL, we examined the binding of avian LpL to a mutant CHO cell line (pgsA-745) that cannot synthesize HSPGs (51). The GPIHBP1-expressing pgsA-745 cells bound 10–20-fold more LpL than cells transfected with empty vector; this binding was saturable, and nonspecific binding was minimal (Figure 21). All of the LpL binding could be released with PIPLC (39). Recently, we also found that GPIHBP1 also binds to *human* LpL, and that this LpL can be released by treatment with PIPLC or heparin (39).

We also tested the binding of fluorescently-labeled chylomicrons to GPIHBP1 on LDL receptor–deficient CHO cells. We found that cells transfected with an empty vector did not bind chylomicrons, whereas the cells transfected with the *Gpihbp1* expression vector bound chylomicrons quite avidly (Figure 22) (39). Chylomicron binding was dramatically reduced by treating the transfected cells with PIPLC (39). The ability of GPIHBP1 to bind both to LpL and to chylomicrons was consistent with our hypothesis that GPIHBP1 plays a critical role in lipolysis, perhaps by drawing chylomicrons and LpL into close proximity along the luminal surface of capillaries (39).

Chylomicrons contain several apolipoproteins (*e.g.*, apo-B48, apo-E, and apo-AV) with positively charged domains; these apolipoproteins are known to bind, *via* electrostatic interactions, to negatively charged molecules such as heparin sulfate or HSPGs (52–54). It is easy to imagine that one or more of these apolipoproteins on chylomicron particles could mediate binding to the strongly negatively charged amino-terminal domain of GPIHBP1.

We imagined that apo-AV could be a good candidate as a ligand for GPIHBP1, since *Apoav* deficiency in mice causes hypertriglyceridemia associated with decreased LpL-mediated lipolysis (55–57). Indeed, our recent experiments have shown, quite unequivocally, that apo-AV–phospholipid disks bind strongly to *Gpihbp1*-transfected cells (39). In the future, it will be interesting to assess the binding of apo-E–phospholipid disks to GPIHBP1.

We have also examined the binding of LpL and chylomicrons to *Gpihbp1*-transfected and nontransfected wild-type CHO-K1 cells (which synthesize HSPGs normally). For LpL, we observed a highly significant 70% increase of binding to the transfected cells compared to non-transfected cells. When comparing CHO-K1 cells and CHO-745 cells both transfected with *Gpihbp1*, CHO-K1 cells bound 60% more LPL. Total binding to the transfected cells reflects binding to *Gpihbp1* and probably also to heparan sulfate chains. For chylomicrons, increased chylomicron binding to the transfected cells was easily detectable. For apo-AV, the levels of binding to the nontransfected cells were very high—so high that differences between *Gpihbp1*-transfected and nontransfected cells were obscured (Dr. Peter Gin, unpublished observations).

It would obviously be desirable to assess binding of all of these ligands to endothelial cells rather than transfected cells. However, preliminary studies suggest that GPIHBP1 is not expressed in aortic endothelial cells or late-passage microvascular endothelial cells from the heart (Dr. Brandon Davies, unpublished observations).

Although GPIHBP1 on the surface of CHO cells clearly has the capability of binding to LpL and chylomicrons *in vitro*, we emphasize that the precise role of GPIHBP1 in lipolysis is incompletely understood. While GPIHBP1 likely acts as a platform for lipolysis, the details are sketchy. One possibility is that GPIHBP1 binds LpL and chylomicrons, and that both of these roles are essential. Another possibility is that the main role of GPIHBP1 is in binding chylomicrons, and that LpL binds secondarily to the lipoproteins, perhaps being recruited from surrounding HSPGs. Still another possibility is that the principal role of GPIHBP1 is the binding of LpL, and that LpL, rather than GPIHBP1 itself, plays a predominant role in binding chylomicrons in the bloodstream.

Might Apo-B48 Play a Role in the Binding of Chylomicrons to GPIHBP1?

Another interesting hypothesis is that GPIHBP1 could act as a receptor for apo-B48, the key structural protein of chylomicrons. Abundant evidence indicates that apo-B48–containing remnants are taken up by liver receptors *via* interactions with apo-E on these particles (28). Thus far, however, there has been little convincing evidence that apo-B48 itself specifically mediates binding to any cell-surface receptor. However, if apo-B48 were to bind directly to GPIHBP1 on the surface of endothelial cells within capillaries, it would make some physiologic sense, as it would provide a mechanism to unload the cargo of apo-B48–containing intestinal lipoproteins (*i.e.*, triglycerides) to physiologically relevant tissues (*i.e.*, muscle and adipose tissue—tissues where GPIHBP1 is expressed).

Both apo-B48 and chylomicrons (defined as intestinal lipoproteins that are initially secreted into the lymph) are found only in mammals (58). Similarly, GPIHBP1 is found in all mammals, including platypus (an aquatic egg-laying mammal), but is absent from the genomes of lower organisms. We suspect that apo-B48 and GPIHBP1 are both mammalian adaptations to optimize the delivery of triglycerides to vital tissues. In the future, we believe that it will be interesting to determine if apo-B48 binds specifically to GPIHBP1. It will also be interesting to determine if the processing of apo-B100–containing lipoproteins is equally dependent on GPIHBP1 and to determine if *Gpihbp1*$^{-/-}$*Apob*$^{100/100}$ mice would manifest equally severe hypertriglyceridemia.

Spontaneous Atherosclerotic Lesions in Chow-fed *Gpihbp1*$^{-/-}$ Mice

We had predicted that the *Gpihbp1*$^{-/-}$ mice on a chow diet would not manifest spontaneous atherosclerotic lesions, simply because the lipoproteins in the plasma of these mice were so immense. However, preliminary observations suggest that *Gpihbp1*$^{-/-}$ mice do indeed develop atherosclerosis (Mr. Michael Weinstein, Drs. Liya Yan, Loren Fong, unpublished observations). If this finding holds up, it would raise several issues. Can large triglyceride-rich lipoproteins somehow drive the formation of atherosclerotic lesions? Is the atherosclerosis in these mice largely dependent on the level of cholesterol in the triglyceride-rich lipoproteins? If so, would the atherosclerosis in these mice be eliminated with ezetimibe? Given the striking delay in the clearance of chylomicrons, would dietary oxidized lipids exhibit a markedly prolonged circulation time? Would oxidized lipids in the diet increase the susceptibility of *Gpihbp1*$^{-/-}$ mice to atherosclerosis? In the future, it would be interesting to address each of these questions.

Acknowledgments

The authors thank many dedicated postdoctoral fellows, students, and research associates for their help with the studies described in this chapter. Supported by grants from the NIH (R01 HL087228 and R01 HL76839) and by a beginning Grant-in-Aid from the American Heart Association, Western States Affiliate.

References

1. Grundy SM. Cholesterol and coronary heart disease. A new era. J Am Med Assoc 1986;256:2849–2858.
2. Brown MS, Goldstein JL. A receptor-mediated pathway for cholesterol homeostasis. Science 1986;232:34–47. [PubMed: 3513311]
3. NIH Consensus Development Panel. Triglyceride, high-density lipoprotein, and coronary heart disease. J Am Med Assoc 1993;269:505–510.
4. Feussner G, Wagner A, Kohl B, Ziegler R. Clinical features of type III hyperlipoproteinemia: Analysis of 64 patients. Clin Investig 1993;71:362–366.
5. Fazio S, Lee Y-L, Ji Z-S, Rall SC Jr. Type III hyperlipoproteinemic phenotype in transgenic mice expressing dysfunctional apolipoprotein E. J Clin Invest 1993;92:1497–1503. [PubMed: 8376602]
6. Brunzell JD, Bierman EL. Chylomicronemia syndrome. Interaction of genetic and acquired hypertriglyceridemia. Med Clin North Am 1982;66:455–468. [PubMed: 7040847]
7. Chait A, Brunzell JD. Chylomicronemia syndrome. Adv Intern Med 1991;37:249–273. [PubMed: 1557997]
8. Benlian P, De Gennes JL, Foubert L, Zhang H, Gagne SE, Hayden M. Premature atherosclerosis in patients with familial chylomicronemia caused by mutations in the lipoprotein lipase gene. N Engl J Med 1996;335:848–854. [PubMed: 8778602]
9. Duff GL, McMillan GC. The effect of alloxan diabetes on experimental cholesterol atherosclerosis in the rabbit. I. The inhibition of experimental cholesterol atherosclerosis in alloxan diabetes. II. The effect of alloxan diabetes on the retrogression of experimental cholesterol atherosclerosis. J Exp Med 1949;89:611–630. [PubMed: 18129862]
10. Nordestgaard BG, Zilversmit DB. Large lipoproteins are excluded from the arterial wall in diabetic cholesterol-fed rabbits. J Lipid Res 1988;29:1491–1500. [PubMed: 3241125]
11. Nordestgaard BG, Zilversmit DB. Comparison of arterial intimal clearances of LDL from diabetic and nondiabetic cholesterol-fed rabbits. Differences in intimal clearance explained by size differences. Arteriosclerosis 1989;9:176–183. [PubMed: 2923574]
12. Nordestgaard BG, Stender S, Kjeldsen K. Reduced atherogenesis in cholesterol-fed diabetic rabbits. Giant lipoproteins do not enter the arterial wall. Arteriosclerosis 1988;8:421–428. [PubMed: 3395278]
13. Paigen B, Morrow A, Brandon C, Mitchell D, Holmes P. Variation in susceptibility to atherosclerosis among inbred strains of mice. Atherosclerosis 1985;57:65–73. [PubMed: 3841001]

14. Ishida, BY.; Paigen, B. Atherosclerosis in the mouse. In: Lusis, AJ.; Sparkes, SR., editors. Genetic Factors in Atherosclerosis: Approaches and Model Systems. Basel: Karger; 1989. p. 189-222.
15. Paigen B, Morrow A, Holmes PA, Mitchell D, Williams RA. Quantitative assessment of atherosclerotic lesions in mice. Atherosclerosis 1987;68:231–240. [PubMed: 3426656]
16. Rubin EM, Krauss RM, Spangler EA, Verstuyft JG, Clift SM. Inhibition of early atherogenesis in transgenic mice by human apolipoprotein AI. Nature 1991;353:265–267. [PubMed: 1910153]
17. Ishibashi S, Brown MS, Goldstein JL, Gerard RD, Hammer RE, Herz J. Hypercholesterolemia in low density lipoprotein receptor knockout mice and its reversal by adenovirus-mediated gene delivery. J Clin Invest 1993;92:883–893. [PubMed: 8349823]
18. Ishibashi S, Goldstein JL, Brown MS, Herz J, Burns DK. Massive xanthomatosis and atherosclerosis in cholesterol-fed low density lipoprotein receptor–negative mice. J Clin Invest 1994;93:1885–1893. [PubMed: 8182121]
19. Piedrahita JA, Zhang SH, Hagaman JR, Oliver PM, Maeda N. Generation of mice carrying a mutant apolipoprotein E gene inactivated by gene targeting in embryonic stem cells. Proc Natl Acad Sci USA 1992;89:4471–4475. [PubMed: 1584779]
20. Zhang SH, Reddick RL, Piedrahita JA, Maeda N. Spontaneous hypercholesterolemia and arterial lesions in mice lacking apolipoprotein E. Science 1992;258:468–471. [PubMed: 1411543]
21. Plump AS, Smith JD, Hayek T, Aalto-Setälä K, Walsh A, Verstuyft JG, Rubin EM, Breslow JL. Severe hypercholesterolemia and atherosclerosis in apolipoprotein E–deficient mice created by homologous recombination in ES cells. Cell 1992;71:343–353. [PubMed: 1423598]
22. Nakashima Y, Plump AS, Raines EW, Breslow JL, Ross R. ApoE-deficient mice develop lesions of all phases of atherosclerosis throughout the arterial tree. Arterioscler Thromb 1994;14:133–140. [PubMed: 8274468]
23. Véniant MM, Kim E, McCormick S, Borén J, Nielsen LB, Raabe M, Young SG. Insights into apolipoprotein B biology from transgenic and gene-targeted mice. J Nutr 1999;129:451S–455S. [PubMed: 10064308]
24. Véniant MM, Pierotti V, Newland D, Cham CM, Sanan DA, Walzem RL, Young SG. Susceptibility to atherosclerosis in mice expressing exclusively apolipoprotein B48 or apolipoprotein B100. J Clin Invest 1997;100:180–188. [PubMed: 9202070]
25. Véniant MM, Sullivan MA, Kim SK, Ambroziak P, Chu A, Wilson MD, Hellerstein MK, Rudel LL, Walzem RL, Young SG. Defining the atherogenicity of large and small lipoproteins containing apolipoprotein B100. J Clin Invest 2000;106:1501–1510. [PubMed: 11120757]
26. Véniant MM, Withycombe S, Young SG. Lipoprotein size and atherosclerosis susceptibility in *Apoe*$^{-/-}$ and *Ldlr*$^{-/-}$ mice. Arterioscler Thromb Vasc Biol 2001;21:1567–1570. [PubMed: 11597927]
27. Véniant MM, Zlot CH, Walzem RL, Pierotti V, Driscoll R, Dichek D, Herz J, Young SG. Lipoprotein clearance mechanisms in LDL receptor–deficient “apo-B48-only” and “apo-B100-only” mice. J Clin Invest 1998;102:1559–1568. [PubMed: 9788969]
28. Ishibashi S, Herz J, Maeda N, Goldstein JL, Brown MS. The two-receptor model of lipoprotein clearance: Tests of the hypothesis in “knockout” mice lacking the low density lipoprotein receptor, apolipoprotein E, or both proteins. Proc Natl Acad Sci USA 1994;91:4431–4435. [PubMed: 8183926]
29. Farese RV Jr, Véniant MM, Cham CM, Flynn LM, Pierotti V, Loring JF, Traber M, Ruland S, Stokowski RS, Huszar D, Young SG. Phenotypic analysis of mice expressing exclusively apolipoprotein B48 or apolipoprotein B100. Proc Natl Acad Sci USA 1996;93:6393–6398. [PubMed: 8692825]
30. Teng B, Burant CF, Davidson NO. Molecular cloning of an apolipoprotein B messenger RNA editing protein. Science 1993;260:1816–1819. [PubMed: 8511591]
31. Linton MF, Farese RV Jr, Chiesa G, Grass DS, Chin P, Hammer RE, Hobbs HH, Young SG. Transgenic mice expressing high plasma concentrations of human apolipoprotein B100 and lipoprotein(a). J Clin Invest 1993;92:3029–3037. [PubMed: 8254057]
32. Purcell-Huynh DA, Farese RV Jr, Johnson DF, Flynn LM, Pierotti V, Newland DL, Linton MF, Sanan DA, Young SG. Transgenic mice expressing high levels of human apolipoprotein B develop

severe atherosclerotic lesions in response to a high-fat diet. J Clin Invest 1995;95:2246–2257. [PubMed: 7738190]

33. Powell-Braxton L, Véniant M, Latvala RD, Hirano K-I, Won WB, Ross J, Dybdal N, Zlot CH, Young SG, Davidson NO. A mouse model of human familial hypercholesterolemia: Markedly elevated low density lipoprotein cholesterol levels and severe atherosclerosis on a low-fat chow diet. Nat Med 1998;4:934–938. [PubMed: 9701246]
34. Neaton JD, Wentworth D. Serum cholesterol, blood pressure, cigarette smoking, and death from coronary heart disease. Overall findings and differences by age for 316 099 white men. Arch Intern Med 1992;152:56–64. [PubMed: 1728930]
35. Linton MF, Atkinson JB, Fazio S. Prevention of atherosclerosis in apolipoprotein E–deficient mice by bone marrow transplantation. Science 1995;267:1034–1037. [PubMed: 7863332]
36. Yang R, Powell-Braxton L, Ogaoawara AK, Dybdal N, Bunting S, Ohneda O, Jin H. Hypertension and endothelial dysfunction in apolipoprotein E knockout mice. Arterioscler Thromb Vasc Biol 1999;19:2762–2768. [PubMed: 10559023]
37. Verreth W, De Keyzer D, Pelat M, Verhamme P, Ganame J, Bielicki JK, Mertens A, Quarck R, Benhabiles N, Marguerie G, Mackness B, Mackness M, Ninio E, Herregods MC, Balligand JL, Holvoet P. Weight-loss-associated induction of peroxisome proliferator-activated receptor-alpha and peroxisome proliferator-activated receptor-gamma correlate with reduced atherosclerosis and improved cardiovascular function in obese insulin-resistant mice. Circulation 2004;110:3259–3269. [PubMed: 15533870]
38. Camus MC, Chapman MJ, Forgez P, Laplaud PM. Distribution and characterization of the serum lipoproteins and apoproteins in the mouse, Mus musculus. J Lipid Res 1983;24:1210–1228. [PubMed: 6631247]
39. Beigneux A, Davies B, Gin P, Weinstein M, Farber E, Qiao X, Peale F, Bunting S, Walzem R, Wong J, Blaner W, Ding Z, Melford K, Wongsiriroj N, Sauvage Fd, Fong L, Bensadoun A, Young S. Glycosylphosphatidylinositol-anchored high density lipoprotein–binding protein 1 plays a critical role in the lipolytic processing of chylomicrons. Cell Metabolism 2007;5:279–291. [PubMed: 17403372]
40. Ioka RX, Kang M-J, Kamiyama S, Kim D-H, Magoori K, Kamataki A, Ito Y, Takei YA, Sasaki M, Suzuki T, Sasano H, Takahashi S, Sakai J, Fujino T, Yamamoto TT. Expression Cloning and Characterization of a Novel Glycosylphosphatidylinositol-anchored High Density Lipoprotein-binding Protein, GPI-HBP1. J Biol Chem 2003;278:7344–7349. [PubMed: 12496272]
41. Acton SL, Scherer PE, Lodish HF, Krieger M. Expression cloning of SR-BI, a CD36-related class B scavenger receptor. J Biol Chem 1994;269:21003–21009. [PubMed: 7520436]
42. Acton S, Rigotti A, Landschulz KT, Xu S, Hobbs HH, Krieger M. Identification of scavenger receptor SR-BI as a high density lipoprotein receptor. Science 1996;271:518–520. [PubMed: 8560269]
43. Brunzell, JD.; Deeb, SS. Familial lipoprotein lipase deficiency, apo C-II deficiency, and hepatic lipase deficiency. In: Scriver, CR.; Beaudet, AL.; Sly, WS.; Valle, D.; Childs, B.; Kinzler, KW.; Vogelstein, B., editors. The Metabolic and Molecular Bases of Inherited Disease. New York: McGraw-Hill; 2001.
44. Strauss JG, Frank S, Kratky D, Hammerle G, Hrzenjak A, Knipping G, von Eckardstein A, Kostner GM, Zechner R. Adenovirus-mediated rescue of lipoprotein lipase-deficient mice. Lipolysis of triglyceride-rich lipoproteins is essential for high density lipoprotein maturation in mice. J Biol Chem 2001;276:36083–36090. [PubMed: 11432868]
45. Weinstock PH, Bisgaier CL, Aalto-Setälä K, Radner H, Ramakrishnan R, Levak-Frank S, Essenburg AD, Zechner R, Breslow JL. Severe hypertriglyceridemia, reduced high density lipoprotein, and neonatal death in lipoprotein lipase knockout mice. Mild hypertriglyceridemia with impaired low density lipoprotein clearance in heterozygotes. J Clin Invest 1995;96:2555–2568. [PubMed: 8675619]
46. Coleman T, Seip RL, Gimble JM, Lee D, Maeda N, Semenkovich CF. COOH-terminal disruption of lipoprotein lipase in mice is lethal in homozygotes, but heterozygotes have elevated triglycerides and impaired enzyme activity. J Biol Chem 1995;270:12518–12525. [PubMed: 7759497]

47. Nguyen AT, Braschi S, Geoffrion M, Fong LG, Crooke RM, Graham MJ, Young SG, Milne R. A mouse monoclonal antibody specific for mouse apoB48 and apoB100 produced by immunizing “apoB39-only” mice with mouse apoB48. Biochim Biophys Acta 2006;1761:182–185. [PubMed: 16551509]
48. Langner CA, Birkenmeier EH, Ben-Zeev O, Schotz MC, Sweet HO, Davisson MT, Gordon JI. The fatty liver dystrophy (fld) mutation. A new mutant mouse with a developmental abnormality in triglyceride metabolism and associated tissue-specific defects in lipoprotein lipase and hepatic lipase activities. J Biol Chem 1989;264:7994–8003. [PubMed: 2722772]
49. Greenwalt DE, Scheck SH, Rhinehart-Jones T. Heart CD36 expression is increased in murine models of diabetes and in mice fed a high fat diet. J Clin Invest 1995;96:1382–1388. [PubMed: 7544802]
50. Cardin AD, Jackson RL, Sparrow DA, Sparrow JT. Interaction of glycosaminoglycans with lipoproteins. Ann NY Acad Sci 1989;556:186–193. [PubMed: 2735658]
51. Lugemwa FN, Esko JD. Estradiol beta-D-xyloside, an efficient primer for heparan sulfate biosynthesis. J Biol Chem 1991;266:6674–6677. [PubMed: 2016281]
52. Cardin AD, Hirose N, Blankenship DT, Jackson RL, Harmony JAK. Binding of a high reactive heparin to human apolipoprotein E: Identification of two heparin-binding domains. Biochem Biophys Res Commun 1986;134:783–789. [PubMed: 3947350]
53. Cardin AD, Barnhart RL, Witt KR, Jackson RL. Reactivity of heparin with the human plasma heparin-binding proteins thrombin, antithrombin III, and apolipoproteins E and B-100. Thromb Res 1984;34:541–550. [PubMed: 6740570]
54. Lookene A, Beckstead JA, Nilsson S, Olivecrona G, Ryan RO. Apolipoprotein A-V-heparin interactions: implications for plasma lipoprotein metabolism. J Biol Chem 2005;280:25383–25387. [PubMed: 15878877]
55. Pennacchio LA, Olivier M, Hubacek JA, Cohen JC, Cox DR, Fruchart JC, Krauss RM, Rubin EM. An apolipoprotein influencing triglycerides in humans and mice revealed by comparative sequencing. Science 2001;294:169–173. [PubMed: 11588264]
56. Calandra S, Oliva CP, Tarugi P, Bertolini S. APOA5 and triglyceride metabolism, lesson from human APOA5 deficiency. Curr Opin Lipidol 2006;17:122–127. [PubMed: 16531747]
57. Grosskopf I, Baroukh N, Lee SJ, Kamari Y, Harats D, Rubin EM, Pennacchio LA, Cooper AD. Apolipoprotein A-V deficiency results in marked hypertriglyceridemia attributable to decreased lipolysis of triglyceride-rich lipoproteins and removal of their remnants. Arterioscler Thromb Vasc Biol 2005;25:2573–2579. [PubMed: 16166565]
58. Teng B, Davidson NO. Evolution of intestinal apolipoprotein B mRNA editing. Chicken apolipoprotein B mRNA is not edited, but chicken enterocytes contain *in vitro* editing enhancement factor(s). J Biol Chem 1992;267:21265–21272. [PubMed: 1400437]

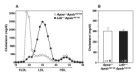

Figure 1.
Lipid and lipoprotein levels in *Apoe*$^{-/-}$*Apob*$^{100/100}$ (*n* = 44) and *Ldlr*$^{-/-}$*Apob*$^{100/100}$ (*n* = 42) mice. (A) Distribution of cholesterol within different lipoprotein fractions. (B) Mean plasma cholesterol levels in *Apoe*$^{-/-}$*Apob*$^{100/100}$ (*n* = 44) and *Ldlr*$^{-/-}$*Apob*$^{100/100}$ (*n* = 42) mice at 40 weeks of age. Reproduced from a paper by Véniant *et al*. (25) with permission from the American Society of Clinical Investigation.

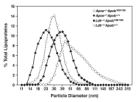

Figure 2.

Lipoprotein sizes in *Apoe*$^{-/-}$*Apob*$^{100/100}$, *Ldlr*$^{-/-}$*Apob*$^{100/100}$, *Ldlr*$^{-/-}$*Apob*$^{+/+}$, and *Apoe*$^{-/-}$*Apob*$^{+/+}$ mice. The median diameter of lipoproteins in *Apoe*$^{-/-}$*Apob*$^{100/100}$ mice (n = 15) was 140% larger than in *Ldlr*$^{-/-}$*Apob*$^{100/100}$ (n = 21) mice, 90% larger than in *Ldlr*$^{-/-}$*Apob*$^{+/+}$ mice (n = 17), and 50% larger than in *Apoe*$^{-/-}$*Apob*$^{+/+}$ mice (n = 16). The size of VLDL (d < 1.006 g/ml) particles ranged from an average of 33.4 nm in *Ldlr*$^{-/-}$*Apob*$^{100/100}$ mice to 61 nm in *Apoe*$^{-/-}$*Apob*$^{100/100}$ mice; the size of IDL (d = 1.006–1.020 g/ml) particles ranged from an average of 27 nm in *Ldlr*$^{-/-}$*Apob*$^{100/100}$ mice to 38 nm in *Apoe*$^{-/-}$*Apob*$^{100/100}$ mice; the size of LDL (d = 1.020–1.052 g/ml) particles was 23 nm in *Apoe*$^{-/-}$*Apob*$^{100/100}$ plasma, 20 nm in *Apoe*$^{-/-}$*Apob*$^{+/+}$ plasma, 22 nm in *Ldlr*$^{-/-}$*Apob*$^{100/100}$ plasma, and 19 nm in *Ldlr*$^{-/-}$*Apob*$^{+/+}$ plasma. The difference in size between the bottom and top deciles of particles was 64.0 nm for *Apoe*$^{-/-}$*Apob*$^{100/100}$ mice, 27.2 nm for *Apoe*$^{-/-}$*Apob*$^{+/+}$ mice, 17.8 nm for *Ldlr*$^{-/-}$*Apob*$^{+/+}$ mice, and 17.0 nm for *Ldlr*$^{-/-}$*Apob*$^{100/100}$ mice. Reproduced from a paper by Véniant *et al*. (25) with permission from the American Society of Clinical Investigation.

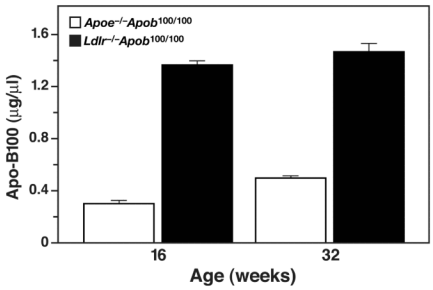

Figure 3.
Apo-B100 levels in *Apoe*$^{-/-}$*Apob*$^{100/100}$ (*n* = 36) and *Apoe*$^{-/-}$*Apob*$^{+/+}$ mice (*n* = 34) at 16 and 32 weeks of age, as judged by a monoclonal antibody–based radioimmunoassay. Reproduced from a paper by Véniant *et al*. (25) with permission from the American Society of Clinical Investigation.

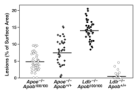

Figure 4.

Morphometric assessment of atherosclerotic lesions in *Apoe*$^{-/-}$*Apob*$^{100/100}$ (*n* = 44), *Apoe*$^{-/-}$*Apob*$^{+/+}$ (*n* = 40), *Ldlr*$^{-/-}$*Apob*$^{100/100}$ (*n* = 42), and *Ldlr*$^{-/-}$*Apob*$^{+/+}$ (*n* = 40) mice. Differences between all groups were significant at the $P < 0.0001$ level with one exception: the lesions in *Apoe*$^{-/-}$*Apob*$^{+/+}$ mice were different from those in *Apoe*$^{-/-}$*Apob*$^{100/100}$ mice at $P = 0.0004$. Reproduced from a paper by Véniant *et al*. (25) with permission from the American Society of Clinical Investigation.

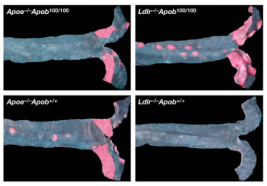

Figure 5.
Representative Sudan IV–stained thoracic aortas. The amount of atherosclerosis in these four aortas matched the mean level for each genotype of mice. Reproduced from a paper by Véniant *et al*. (25) with permission from the American Society of Clinical Investigation.

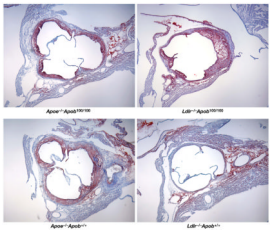

Figure 6.
Oil Red O–stained sections of proximal aortic roots for different mouse genotypes. Reproduced from a paper by Véniant *et al.* (25) with permission from the American Society of Clinical Investigation.

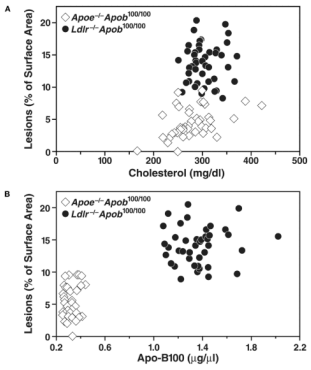

Figure 7.

Relationship between atherosclerotic lesions and the total plasma cholesterol levels and plasma apo-B100 levels in *Apoe*$^{-/-}$*Apob*$^{100/100}$ (*n* = 41) and *Ldlr*$^{-/-}$*Apob*$^{100/100}$ (*n* = 40) mice. The top panel shows a plot of lesions, as assessed by morphometric techniques, *versus* total plasma cholesterol levels (mean of the five measurements). The bottom panel shows a plot of lesions *versus* the plasma apo-B100 levels (measured at 32 weeks). Reproduced from a paper by Véniant *et al*. (25) with permission from the American Society of Clinical Investigation.

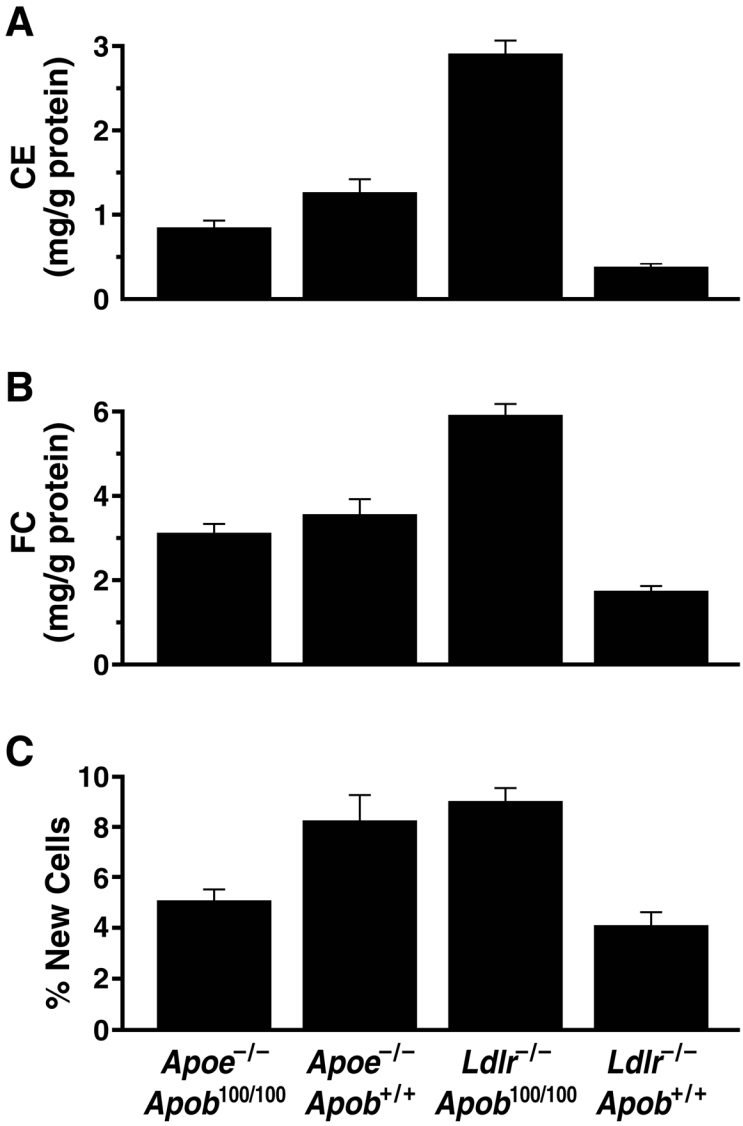

Figure 8.

Scoring of aortic pathology in the four groups of mice according to the aortic content of free and esterified cholesterol and aortic DNA synthesis rate. (A) Cholesterol ester content of aortas in *Apoe*$^{-/-}$*Apob*$^{100/100}$ (n = 43), *Apoe*$^{-/-}$*Apob*$^{+/+}$ (n = 38), *Ldlr*$^{-/-}$*Apob*$^{100/100}$ (n = 39), and *Ldlr*$^{-/-}$*Apob*$^{+/+}$ (n = 34) mice. (B) Free cholesterol content of aortas in the four different groups of mice (numbers of mice identical to those for panel A). (C) Aortic DNA synthesis rates in *Apoe*$^{-/-}$*Apob*$^{100/100}$ (n = 18), *Apoe*$^{-/-}$*Apob*$^{+/+}$ (n = 17), *Ldlr*$^{-/-}$*Apob*$^{100/100}$ (n = 25), and *Ldlr*$^{-/-}$*Apob*$^{+/+}$ (n = 14) mice. Reproduced from a paper by Véniant *et al*. (25) with permission from the American Society of Clinical Investigation.

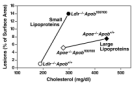

Figure 9.

Mean extent of atherosclerotic lesions plotted against the mean total plasma cholesterol level. The atherosclerosis data (assessed by morphometric techniques) and the cholesterol data represent means calculated from all of the mice in each group. The steep increase in atherosclerosis in LDL receptor–deficient mice between total cholesterol concentrations of ~200 and ~300 mg/dl suggests that small LDL particles are particularly atherogenic. Reproduced from a paper by Véniant *et al*. (25) with permission from the American Society of Clinical Investigation.

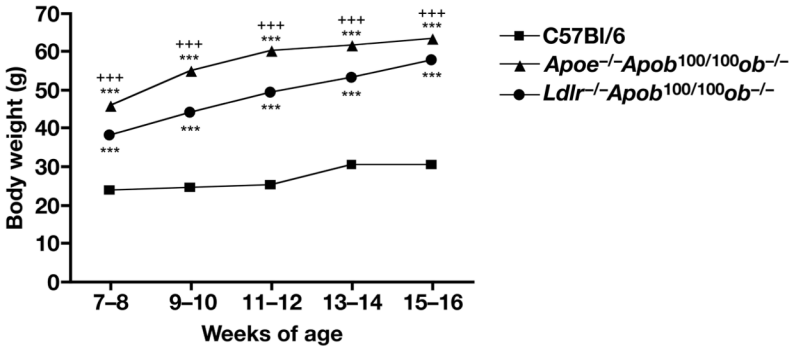

Figure 10.

Body weight in *Apoe*$^{-/-}$*Apob*$^{100/100}$*ob*$^{-/-}$ (n = 18–52) and *Ldlr*$^{-/-}$*Apob*$^{100/100}$ *ob*$^{-/-}$ (n = 22–52) mice. Body weights were significantly increased in *Apoe*$^{-/-}$*Apob*$^{100/100}$*ob*$^{-/-}$ and *Ldlr*$^{-/-}$*Apob*$^{100/100}$ *ob*$^{-/-}$ mice compared with wild-type C57BL/6 mice ($P < 0.001$ for both groups).

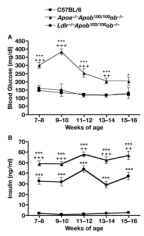

Figure 11.

Blood glucose and insulin levels in *Apoe*$^{-/-}$*Apob*$^{100/100}$*ob*$^{-/-}$ (*n* = 10–24) and *Ldlr*$^{-/-}$*Apob*$^{100/100}$ *ob*$^{-/-}$ (*n* = 5–17) mice. (A) Fed blood glucose levels were significantly higher in *Apoe*$^{-/-}$*Apob*$^{100/100}$*ob*$^{-}$ mice than in wild-type C57BL/6 mice (*P* values at different ages range from 0.05 to 0.001). (B) Fed insulin levels in *Apoe*$^{-/-}$*Apob*$^{100/100}$*ob*$^{-/-}$ and *Ldlr*$^{-/-}$*Apob*$^{100/100}$ *ob*$^{-/-}$ mice (*n* = 16–32). $^{++}P < 0.01$ *vs. Ldlr*$^{-/-}$*Apob*$^{100/100}$ *ob*$^{-/-}$ mice, $^{+++}P < 0.001$ *vs. Ldlr*$^{-/-}$*Apob*$^{100/100}$ *ob*$^{-/-}$ mice, ***$P < 0.001$ *vs.* C57BL/6 mice. Shown are means ± SEM.

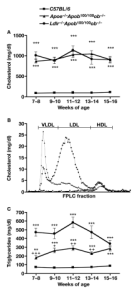

Figure 12.

Plasma lipid levels and lipoprotein profiles in *Apoe*$^{-/-}$*Apob*$^{100/100}$*ob*$^{-/-}$ and *Ldlr*$^{-/-}$*Apob*$^{100/100}$*ob*$^{-/-}$ mice. (A) Cholesterol levels in *Apoe*$^{-/-}$*Apob*$^{100/100}$*ob*$^{-/-}$, *Ldlr*$^{-/-}$*Apob*$^{100/100}$ *ob*$^{-/-}$, and C57BL/6 mice (n = 7–16). (B) Distribution of cholesterol in the plasma lipoproteins of *Apoe*$^{-/-}$*Apob*$^{100/100}$*ob*$^{-/-}$, *Ldlr*$^{-/-}$*Apob*$^{100/100}$ *ob*$^{-/-}$, and wild-type C57BL/6 mice. A total of 2–5 μl of fresh plasma was used for HPLC-fractionation of the plasma. (C) Triglyceride levels in *Apoe*$^{-/-}$*Apob*$^{100/100}$*ob*$^{-/-}$, *Ldlr*$^{-/-}$*Apob*$^{100/100}$*ob*$^{-/-}$, and C57BL/6 wild-type control mice (n = 7–18).

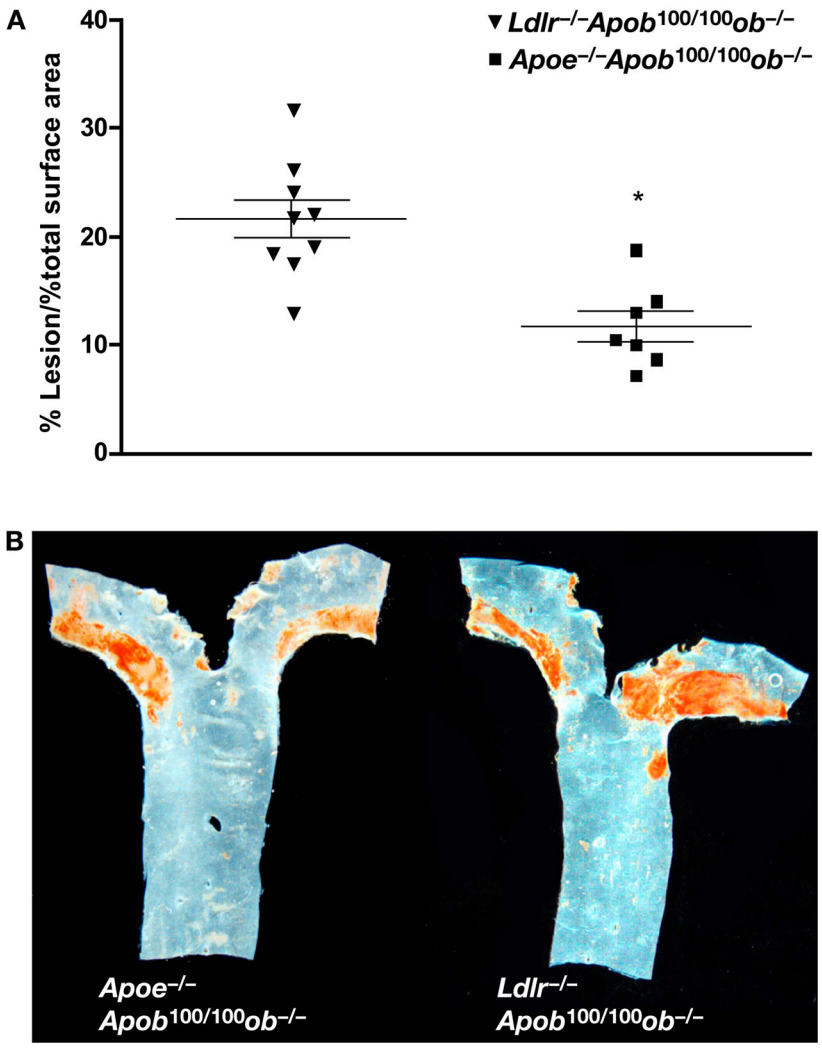

Figure 13.

Atherosclerosis in *Apoe*$^{-/-}$*Apob*$^{100/100}$*ob*$^{-/-}$ and *Ldlr*$^{-/-}$*Apob*$^{100/100}$*ob*$^{-/-}$ mice. (A) The percentage of the aorta occupied by lesions was quantified in *Apoe*$^{-/-}$*Apob*$^{100/100}$*ob*$^{-/-}$ (n = 7) and *Ldlr*$^{-/-}$*Apob*$^{100/100}$*ob*$^{-/-}$ mice (n = 13) after 24 weeks on a chow diet. (B) Representative Sudan IV–stained aortas from a *Apoe*$^{-/-}$*Apob*$^{100/100}$*ob*$^{-/-}$ mouse and a *Ldlr*$^{-/-}$*Apob*$^{100/100}$*ob*$^{-/-}$ mouse.

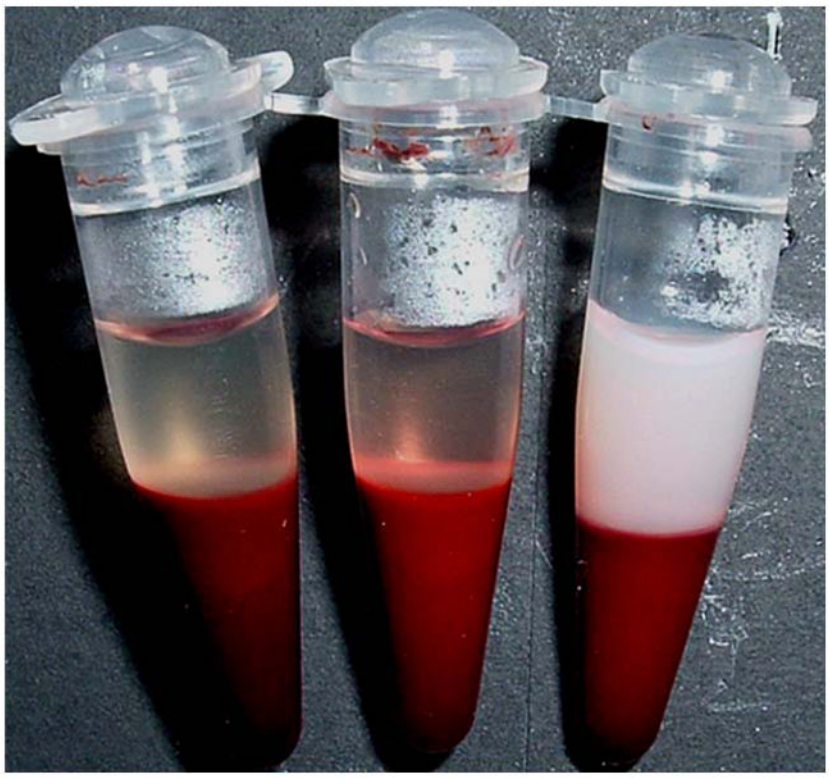

Figure 14.
Plasma samples after low-speed centrifugation. On the right, lipemic plasma from a *Gpihbp1*-deficient mouse. The two samples on the left were from unaffected littermates. Reproduced, with permission from Elsevier, from the article by Beigneux and coworkers (39).

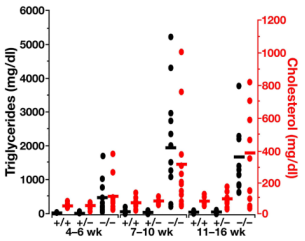

Figure 15.

Plasma triglyceride levels in *Gpihbp1*$^{+/+}$, *Gpihbp1*$^{+/-}$, and *Gpihbp1*$^{-/-}$ mice at different ages, showing higher triglyceride levels in *Gpihbp1*$^{-/-}$ mice ($P < 0.0001$ for each age group). Lipid levels in *Gpihbp1*$^{+/+}$ and *Gpihbp1*$^{+/-}$ mice were not different. Reproduced, with permission from Elsevier, from the article by Beigneux and coworkers (39).

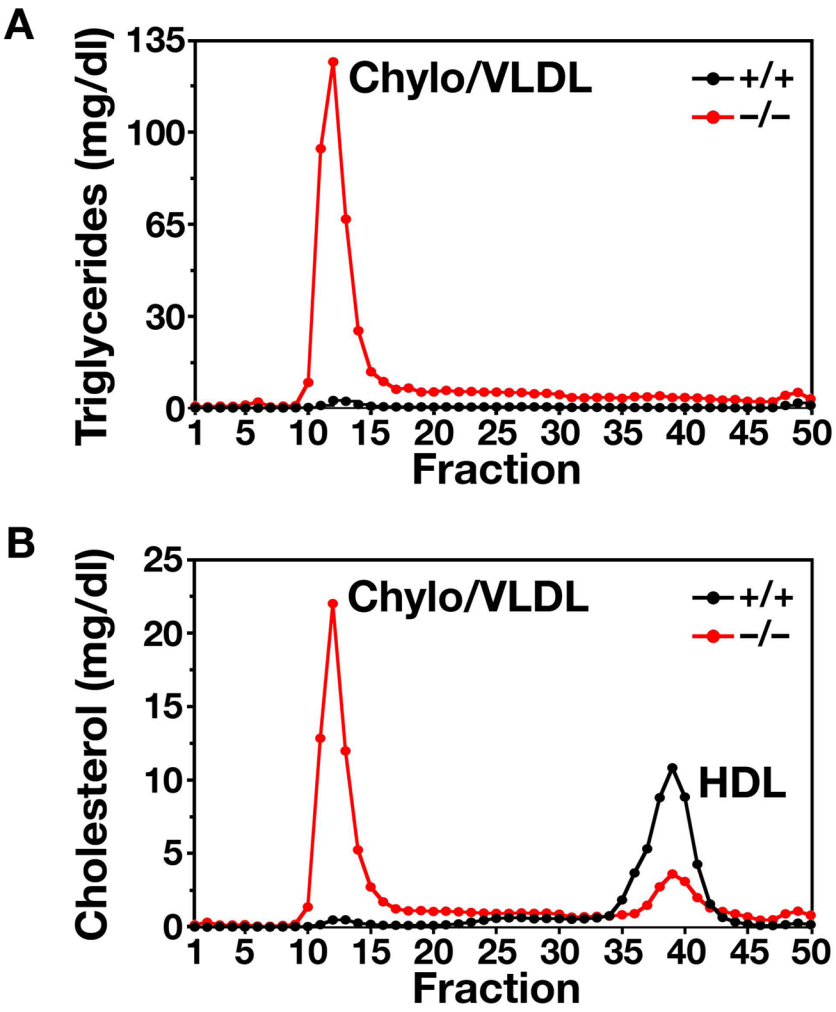

Figure 16.

Distribution of triglyceride and cholesterol in lipoproteins from *Gpihbp1*$^{-/-}$ mice. (A) Distribution of triglycerides in the plasma lipoproteins of *Gpihbp1*$^{+/+}$ and *Gpihbp1*$^{-/-}$ mice. Plasma lipoproteins were separated by size on a Superose 6 FPLC column. (B) Distribution of cholesterol in the plasma lipoproteins of *Gpihbp1*$^{+/+}$ and *Gpihbp1*$^{-/-}$ mice. Reproduced, with permission from Elsevier, from the article by Beigneux and coworkers (39).

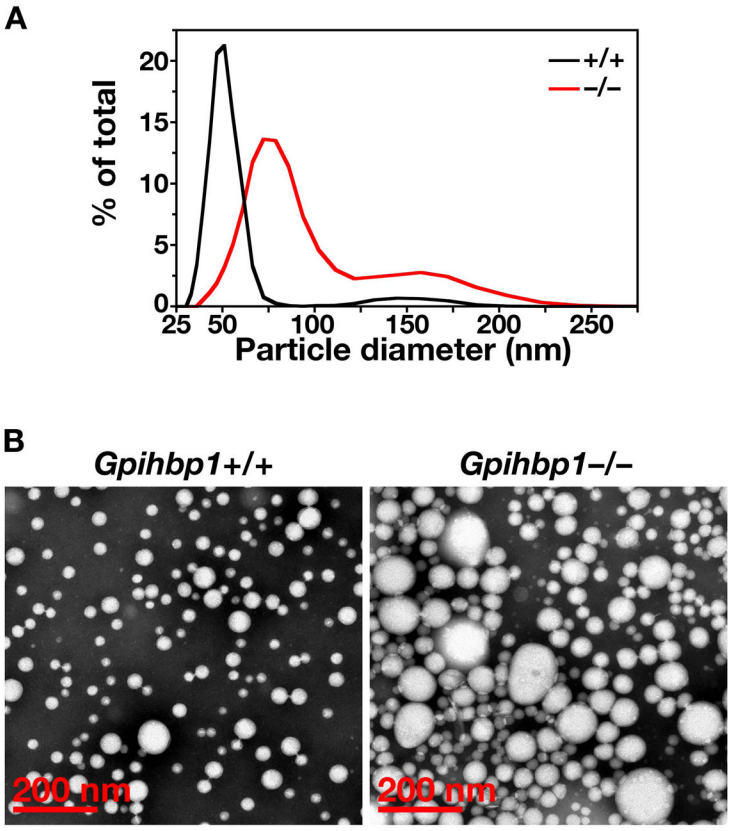

Figure 17.

Distribution of lipoprotein diameters in the $d < 1.022$ g/ml lipoproteins from *Gpihbp1*$^{-/-}$ and *Gpihbp1*$^{+/+}$ mice. (A) As judged by dynamic laser light scattering, the median diameter of lipoproteins was 157% larger in *Gpihbp1*$^{-/-}$ mice ($n = 3$) than in *Gpihbp1*+/+ mice ($n = 6$). 15.4% of the particles in *Gpihbp1*$^{-/-}$ mice had diameters of 122–289 nm. The smaller subpopulation of particles in *Gpihbp1*$^{-/-}$ mice had diameters of 39–111 nm. (B) Electron micrographs of negatively stained $d < 1.006$ g/ml lipoproteins from the plasma of *Gpihbp1*$^{-/-}$ and *Gpihbp1*$^{+/+}$ mice, showing larger lipoproteins in *Gpihbp1*$^{-/-}$ mice. Reproduced, with permission from Elsevier, from the article by Beigneux and coworkers (39).

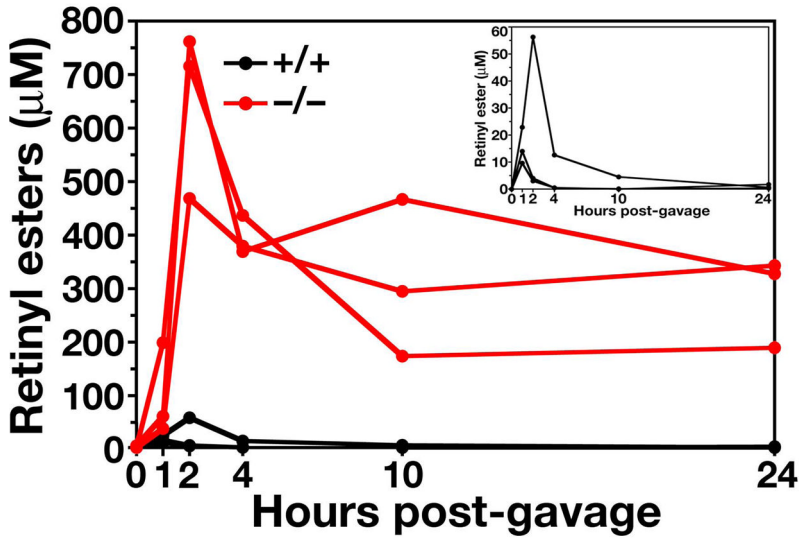

Figure 18.

Delayed clearance of retinyl esters in *Gpihbp1*$^{-/-}$ mice. Retinyl palmitate (5000 IU in 50 μl of vegetable oil) was administered by gavage, and retinyl esters in the plasma were measured over the next 24 h. Inset: retinyl ester levels in *Gpihbp1*$^{+/+}$ mice, plotted on a different scale, peaked between 1 and 2 h and had largely disappeared by 10 h. Reproduced, with permission from Elsevier, from the article by Beigneux and coworkers (39).

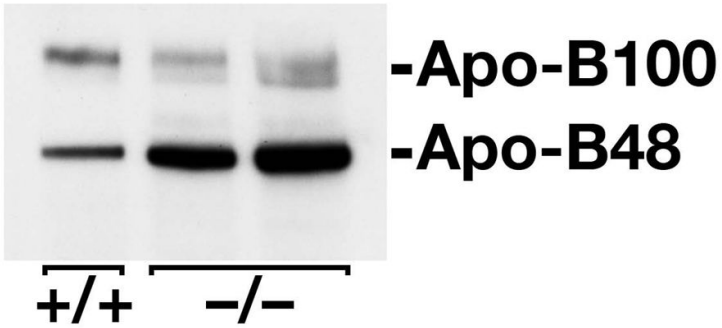

Figure 19.
Western blot of mouse plasma (1.0 μl) with a mouse apo-B–specific monoclonal antibody, showing increased amounts of apo-B48 in the plasma of *Gpihbp1*$^{-/-}$ mice. Reproduced, with permission from Elsevier, from the article by Beigneux and coworkers (39).

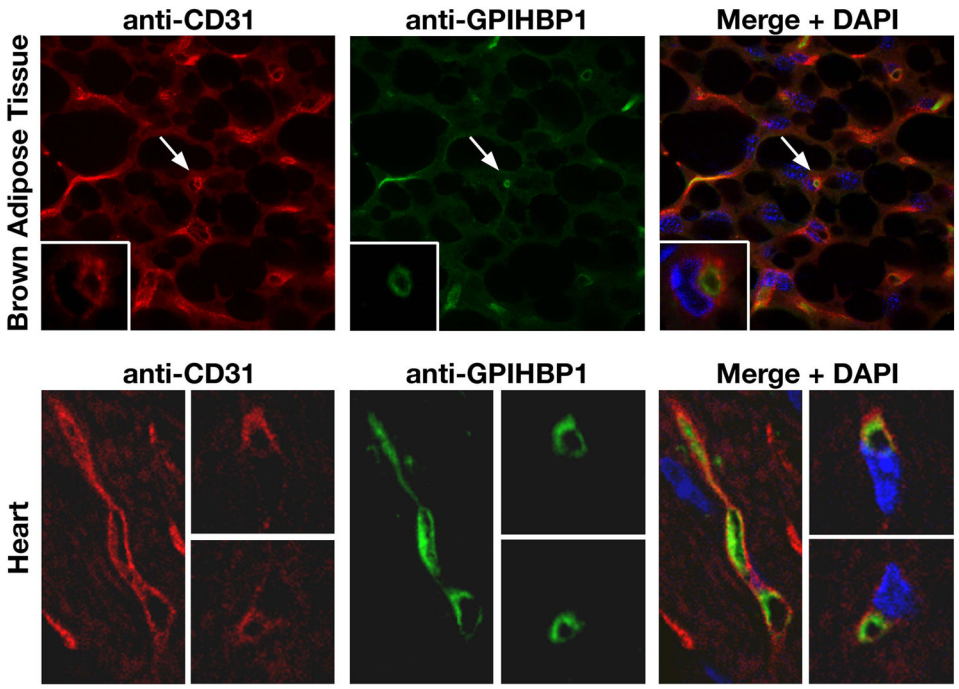

Figure 20.

GPIHBP1 is located within the lumen of the capillary endothelium of brown adipose tissue and heart. (A) Confocal microscopy showing the binding of antibodies against CD31 and GPIHBP1 to brown adipose tissue from a *Gpihbp1*$^{+/+}$ mouse. Images were taken with a 100× objective. Arrows indicate a capillary shown at higher magnification in the insets (100× objective with 4× digital zoom). Insets: In cross-sections of a capillary, GPIHBP1 staining is particularly prominent on the luminal side. (B) Confocal microscopy showing the binding of antibodies against CD31 and GPIHBP1 to heart tissue from a *Gpihbp1*$^{+/+}$ mouse. GPIHBP1 staining is particularly prominent on the luminal face of the capillary endothelium. Images were taken with a 100× objective. Reproduced, with permission from Elsevier, from the article by Beigneux and coworkers (39).

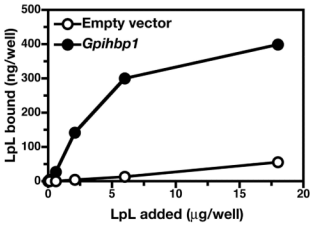

Figure 21.

Testing the ability of cell lines expressing GPIHBP1 to bind LpL. (A) Binding of LpL to pgsA-745 CHO cells stably transfected with a cDNA encoding mouse *Gpihbp1* or empty vector. Cells were incubated for 2 h with increasing amounts of avian LpL. Bound LpL was analyzed by ELISA. The binding of avian LpL to pgsA-745 CHO cells could be eliminated by treating the cells with a phosphatidylinositol-specific phospholipase C. Reproduced, with permission from Elsevier, from the article by Beigneux and coworkers (39).

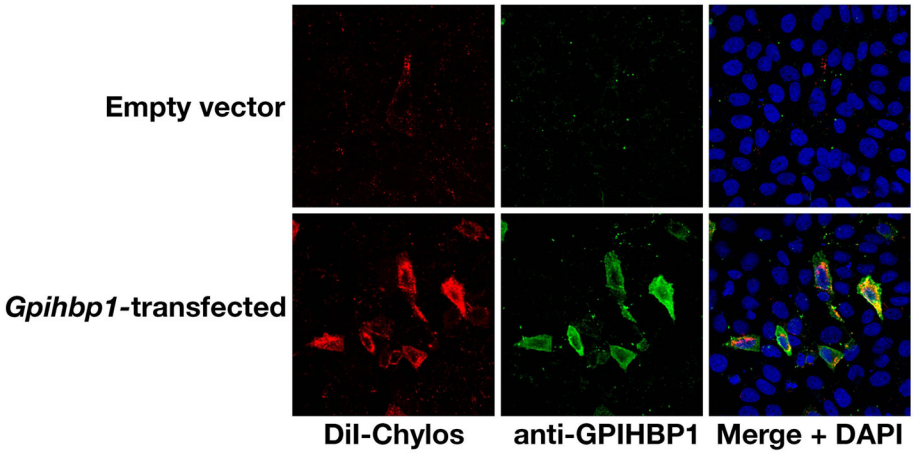

Figure 22.

Binding of DiI-labeled chylomicrons (red) to nonpermeabilized CHO-ldlA7 cells that had been transiently transfected with a mouse *Gpihbp1* cDNA. Binding was measured at 4° C. GPIHBP1 expression was detected with rabbit anti-GPIHBP1 antiserum and FITC-labeled anti-rabbit IgG (green). Reproduced, with permission from Elsevier, from the article by Beigneux and coworkers (39).